AD-A177 280 A STUDY OF THE IDENTIFICATION AND DEVELOPMENT OF PRECIPITATION USING DUAL..(U) UNIVERSITY OF MANCHESTER INST OF SCIENCE AND TECHNOLOGY (ENGL..A J ILLINGWORTH 1/1

UNCLASSIFIED 30 JUN 86 AFOSR-TR-87-0010 AFOSR-85-0188 F/G 17/9 NL

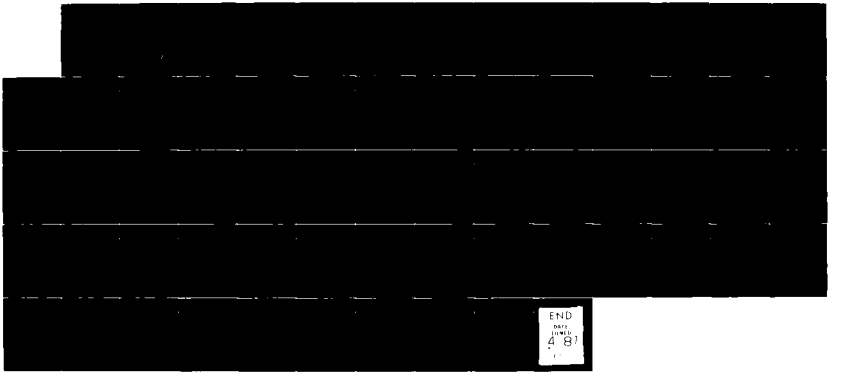

END
DATE FILMED
4 87

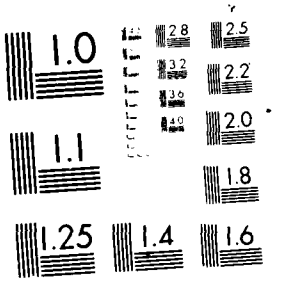
1.0
1.1
1.25
1.4
1.6
1.8
2.0
2.2
2.5
2.8
3.2
3.6
4.0

2

A STUDY OF THE IDENTIFICATION AND DEVELOPMENT OF PRECIPITATION USING DUAL POLARIZATION RADAR

Contract N° AFOSR 85-0188

A STUDY OF THE IDENTIFICATION AND DEVELOPMENT OF PRECIPITATION USING DUAL POLARIZATION RADAR

Contract N° AFOSR 85-0188

Dr A J Illingworth
Physics Department
UMIST
Manchester M60 1QD
England

June 1986

Final Scientific Report 1 May 1985 - 30 April 1986

Approved for public release: distribution unlimited

Prepared for

EUROPEAN OFFICE OF AEROSPACE RESEARCH AND DEVELOPMENT

London England

UNCLASSIFIED
SECURITY CLASSIFICATION OF THIS PAGE

REPORT DOCUMENTATION PAGE

Form Approved OMB No 0704-0188

1a REPORT SECURITY CLASSIFICATION: UNCLASSIFIED	1b RESTRICTIVE MARKINGS:
2a SECURITY CLASSIFICATION AUTHORITY	3 DISTRIBUTION/AVAILABILITY OF REPORT: Approved for public release; distribution unlimited.
2b DECLASSIFICATION/DOWNGRADING SCHEDULE	
4 PERFORMING ORGANIZATION REPORT NUMBER(S)	5 MONITORING ORGANIZATION REPORT NUMBER(S)
6a NAME OF PERFORMING ORGANIZATION: Univ of Manchester Institute of Science and Tech; 6b OFFICE SYMBOL (If applicable):	7a NAME OF MONITORING ORGANIZATION: AFOSR/NC
6c ADDRESS (City, State, and ZIP Code): Department of Physics, Sackville Street, Manchester M60 1QD, England	7b ADDRESS (City, State, and ZIP Code): Building 410, Bolling AFB, DC 20332-6448
8a NAME OF FUNDING/SPONSORING ORGANIZATION: AFOSR; 8b OFFICE SYMBOL (If applicable): NC	9 PROCUREMENT INSTRUMENT IDENTIFICATION NUMBER: AFOSR-85-0188
8c ADDRESS (City, State, and ZIP Code): Building 410, Bolling AFB, DC 20332-6448	10 SOURCE OF FUNDING NUMBERS: PROGRAM ELEMENT NO 61102F; PROJECT NO 2310; TASK NO A1; WORK UNIT ACCESSION NO

11 TITLE (Include Security Classification): A Study Of The Identification And Development Of Precipitation Using Dual Polarization Radar (U)

12 PERSONAL AUTHOR(S): Illingworth, Anthony John

13a TYPE OF REPORT	13b TIME COVERED	14 DATE OF REPORT (Year, Month, Day)	15 PAGE COUNT
Final	FROM 04/85 TO 05/86	86 June 30	62

16 SUPPLEMENTARY NOTATION

17 COSATI CODES		
FIELD	GROUP	SUB-GROUP

18 SUBJECT TERMS (Continue on reverse if necessary and identify by block number): Polarization Radar, Hail, Raindrops.

19 ABSTRACT (Continue on reverse if necessary and identify by block number)

Dual polarization radar measures the shape of precipitation particles within clouds. Analysis of such radar data is described in three papers. The first paper summarises a method which enables hail to be identified by radar for the first time. The exact shape of large raindrops in heavy rain is not known precisely, but is needed for radar estimates of rainfall, and the second paper, based on a statistical analysis of radar data, deduces that they are more oblate than previously suggested. The third paper concludes that large supercooled raindrops, rather than ice, are present in rapidly developing convective clouds. Work to be carried out in the summer and fall of 1986 is outlined.

20 DISTRIBUTION/AVAILABILITY OF ABSTRACT	21 ABSTRACT SECURITY CLASSIFICATION	
☒ UNCLASSIFIED/UNLIMITED ☒ SAME AS RPT ☐ DTIC USERS	UNCLASSIFIED	
22a NAME OF RESPONSIBLE INDIVIDUAL: James P. Koermer, Lt Col, USAF	22b TELEPHONE (Include Area Code): (202) 767-4960	22c OFFICE SYMBOL: NC

DD Form 1473, JUN 86 — Previous editions are obsolete. — SECURITY CLASSIFICATION OF THIS PAGE: UNCLASSIFIED

TABLE OF CONTENTS

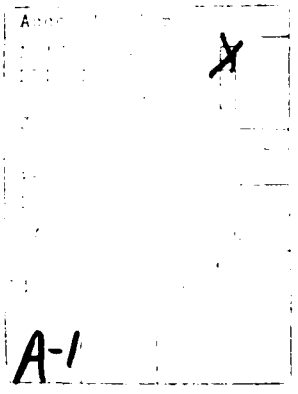

1. INTRODUCTION

The radar reflectivity, Z, measured by conventional meteorological radars does not provide any indication of the type of hydrometeor present in the cloud, and is consequently unable to differentiate between liquid raindrops and the various forms of solid precipitation. It can give no direct indication of whether damaging hail is present within a storm.

It is customary to interpret the magnitude of the reflectivity, Z, in terms of a rainfall rate, R. Various empirical relationships exist between Z and R, but in any particular storm the rainfall rate derived from Z alone may be in error by up to 50%. This error arises because Z, for raindrops, is proportional to ND^6, where N is the concentration of particles of diameter D, summed over all drop sizes. The same Z can arise from different drop size distributions which would have very different rainfall rates. For example the same Z would be observed for one particle of size one cm and 10^{12} drizzle drops of diameter 0.1mm.

The differential reflectivity measurement, ZDR, is able to remove many of these ambiguities. It provides an indication of hydrometeor type and is able to provide a measure of the raindrop size distribution and so leads to more accurate estimates of rainfall rate. This information is of use in predicting the attenuation of communication links by precipitation, for identifying potentially hazardous regions of clouds, and appears to have some predictive value in identifying clouds which are likely to grow explosively in the space of a few minutes.

In essence, the technique involves comparing the radar reflectivity (ZH) measured using horizontally polarised radiation with the reflectivity (ZV) sensed using vertically polarised radiation. The differential reflectivity, ZDR, is defined as:

$$ZDR = 10 \log (ZH/ZV).$$

Small raindrops are spherical and so have equal values of ZH and ZV and give rise to zero values of ZDR. As the raindrops become larger they become increasingly oblate and so ZH becomes larger than ZV, ZDR (in dB) becomes positive, and its magnitude is a measure of the mean size of the raindrops. The Z and ZDR information can then be used to estimate the raindrop size distribution, and so provide a more accurate estimate of the rainfall rate than is possible with Z alone.

The interpretation of the ZDR of ice is rather more complicated because the shape of ice particles is not a unique function of their size. If the ice particles tumble as they fall, as is usually the case within convective clouds, then although for an individual particle ZH and ZV may be unequal, on the average the two reflectivities are the same, the value of ZDR in areas colder than freezing is usuallly close to zero. In stratiform clouds the situation is rather different. Values of Z are lower than in convective clouds, but some regions of positive ZDR are observed. This positive ZDR is believed to be due to small single crystals of ice, such as needles or plates, which have their horizontal diameter greater than the vertical and which fall without tumbling.

During the first year of this researach project the principal task has been the analysis of Z and ZDR measurements made in both convective and stratiform clouds. The appendix contains three papers which describe the work in detail, one is already published, a second is to be presented at the forthcoming Radar Meteroolgy conference, and the third has been submitted for publication. The subject of the first paper is the use of Z and ZDR for identification of hail and is discussed in Section 2. The precise shape of raindrops of various sizes is of crucial importance in interpreting the ZDR of rain in terms of a mean raindrop size; an exhaustive statistical study of the variation of Z with ZDR suggests that raindrops are rather more oblate than the previously accepted shapes. This work is described in Section 3 and appendix B. In Section 4 of this report (and in greater detail in the paper in appendix C) we analyse the evolution of convective clouds. We conclude that the precipitation in vigorously growing convective clouds appears to grow via the coalescence of supercooled droplets and not via the ice phase. Such clouds contain unexpectedly large supercooled raindrops which could be hazardous to aviation, and would also cause anomalously high attenuation of em radiation.

2 HAIL DETECTION

Hail is one of the most dangeroues aspects of convective storms. In the past several radar techniques have been suggested to identify hail, but all have been found to be unsatisfactory. The dual polarisation radar technique appears reliably to be able to identify hail within clouds. The brief note to Nature in appendix A describes the technique. In essence hail only occurs in fairly vigorous showers having reflectivities above 50dBZ. Near to the ground the precipitation is usually in the form of heavy rain which would have a fairly large mean drop size; these large oblate drops would result in an observed value of ZDR always exceeding 1dB. However hailstones tumble as they fall and and thus result in a zero ZDR value. Both heavy rain and hail will be associated with high values of Z, but any hail should give rise to zero ZDR and be clearly distinguishable from the surrounding heavy rain which has positive ZDR. This is illustrated in figure 1, which is a vertical section in Z and ZDR through a vigrous convective cloud. Below 2km altitude the values of Z are generally positive when Z is above 30dBZ, as would be expected for any reasonable drop size distribution. In contrast to this is a region at 87km range where zero values of ZDR extend right down to the ground. If this was due to small spherical raindrops then the computed rainfall rates would be several meters an hour, and the only plausible explanation is that the particles are tumbling hailstones, which are so large that they reach the ground without melting appreciably.

2. PROPOSED NEW RAINDROP SHAPES

The shape of raindrops is critical in the interpretation of the ZDR data. Gans scattering theory is used to calculate the values of ZH and ZV expected for oblate spheroids having various axial ratios. The Chilbolton radar is able to measure ZDR to 0.1dB which is equivalent to a change in axial ratio of about 0.01. This change is less than the error in the best laboratory

measurements of axial ratios by Pruppacher and Pitter. Earlier work at Chilbolton had suggested a small change in the proposed drop shapes of less than the errors of the laboratory measurements, so that the Z and ZDR observed with the radar would agree with the drop sizes measured directly at the ground just 200m below the radar beam and remove a small sytematic error..

However there is considerable uncertainty as to the precise shapes of drops having an equivalent diameter above 4mm. Direct verification is difficult. In the laboratory the precise shape and degree of oscillation of such large drops will vary wth the degree of turbulence in the wind tunnel. In the field the number of occasions when such heavy rain falls directly over the ground based measuring system is small.

We have adopted a statistical approach. It is known that on the average, the concentration of raindrops (N) of size D follows the Marshall-Pallmer size distribution:

$$N(D) = No \exp(-3.67\ Do/D)$$

where No and Do are constants. By summing the contributions of the various differently sized drops to ZH and ZV we can compute how we expect ZDR to increase as the rainfall rate increases and Z becomes larger. This is shown in Figure 2 where the dotted curve marked P is for the predicted average variation of Z with ZDR using the widely accepted raindrop shapes of Pruppacher ad Pitter. According to these curves any value of ZDR above 3.5dB cannot be interpreted in terms of raindrops and we must invoke some very distorted half melted hail pellets. A very limited series of measurements made by Cooper et al using 2D probes to measure the shape of larger drops suggested a deviation from this form, and the dotted curve C has been computed by extrapolating their limited measurements. The solid curve is the average of 90000 data points observed by the radar on eight different days during the summer of 1983. This seems to demonstrate that indeed the larger raindrops are much more oblate than suggested by the laboratory experiments.

There are several implications for the radar work. First, values of ZDR of up to 6dB can be explained in terms of raindrops instead of needing to invoke extraordinarily distorted melting particles. Second, the rainfall rates and drop concentrations in heavy thunderstorm type rain are quite dependent upon the precise shape of the larger drops, for values of Z near 60dBZ the two models predict raindrop oncentrations differing by an order of magnitude. Finally these more oblate drop shapes will lead to different attenuation on microwave links than that predicted by the previous models. A nore detailed description is given in appendix B.

4. STUDIES OF CONVECTIVE PRECIPITATION DEVELOPMENT.

An analysis of the rapid development of convective clouds observed in 1983 has been completed and the rather lengthy paper describing this work is included as appendix C. Here we summarise the conclusions from this work:

a) Isolated first echoes having low Z but accompanied by large positve differential reflectivity (ZDR) are likely to intensify very rapidly.

b) These anomalous low Z / high ZDR first echoes indicate the presence of very low concentrations of supercooled raindrops having diameters of several millimeters, which have grown in the absence of ice. Present theories of precipitation development do not predict the appearance of such large supercooled raindrops.

c) Such low concentrations of large drops could be very efficient hail embryos growing to large hailstones after freezing because of the lack of competition for the cloud wter. This may relax the condition for embryo sorting.

d) Columns of positive ZDR extending above the zero degree isotherm occur quite frequently during vigorous corvection. They coincide with periods when the echo is moving upwards at about 10m/s and tend to precede high values of Z.

5 PROGRAM FOR THE SUMMER AND FALL OF 1986

The radar is being modified to measure additional polarisation parameters. At present (June 1986) it is envisaged that it will be operational by the end of July 1986. One extra parameter is the linear depolarisation ratio (LDR) defined as

$$LDR = 10 \log (ZHV/ZV)$$

where ZHV is the power received in the horizontal for transmission in the vertical. In essence LDR provides a measure of the fall mode of the precipitation particles. Raindrops fall with their figure axis aligned in the vertical and so should have a very low value of LDR, but ice particles which tumble will have a finite orthogonal return. The second parameter is the pulse to pulse fluctuation in ZDR, which we call SDR, which should give an indication of the width of the size distribution of the particles. for monodispersed particles ZDR does not fluctuate and SDR should be zero, finite values of SDR suggest a wide distribution of particle sizes are present.

We initially propose the following tasks:

a) Further work on tracking hail cells using both the ZDR and the proposed LDR signature.

b) Confirmation in widespread rain that the LDR of rain is indeed very low and can be used as an additional means of distinguishing rain from ice.

c) Supercooled raindrops in vigorous convection. Confirmation using LDR that these particles are indeed raindrops.

d) LDR measurement of the ice in convective clouds, ZDR is zero indicating tumbling particles which should therefore have a measurable LDR return.

FIGURE 1

A) THE RADAR REFLECTIVITY, Z, in dBZ above $1mm^6m^{-3}$.

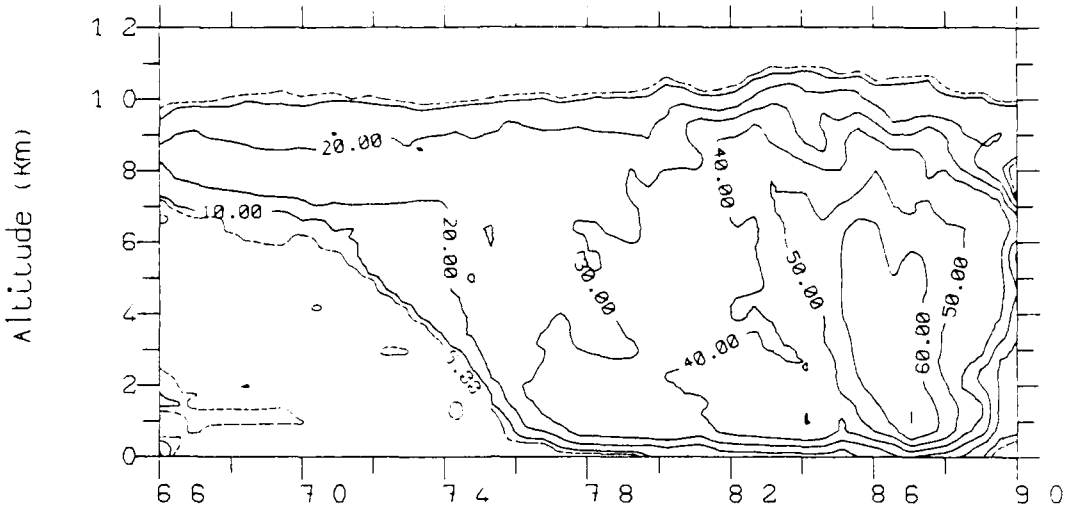

B) THE DIFFERENTIAL RADAR REFLECTIVITY, Z_{DR}, in dB.

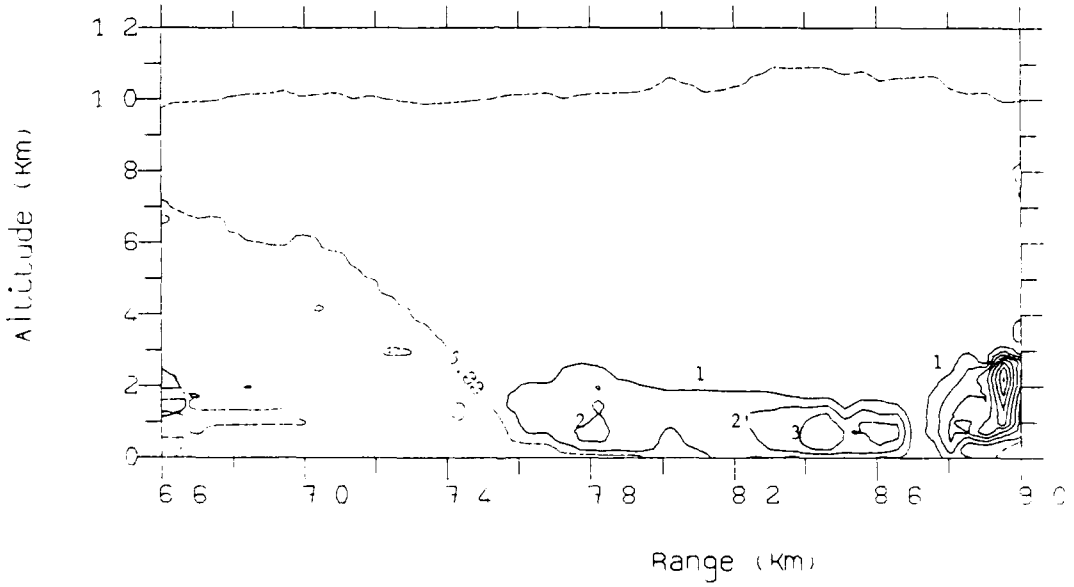

A vertical scan obtained on 6 July 1983 at 1336 UT through an intense convective storm. In A) contours of Z are drawn every 10dBZ with an additional dotted 5dBZ contour. In B) the contours of differential reflectivity, Z_{DR}, are plotted at 1dB intervals starting at 1dB, together with the dotted 5dBZ contour from A) which serves to delineate the extent of the echo. The positive values of Z_{DR} below 2km altitude are due to raindrops falling with their horizontal axis larger than the vertical. In contrast to this at 87km range is a narrow region less than 1km wide where zero Z_R extends down to the ground. It is believed that this is due to tumbling hail falling to the ground.

FIGURE 2

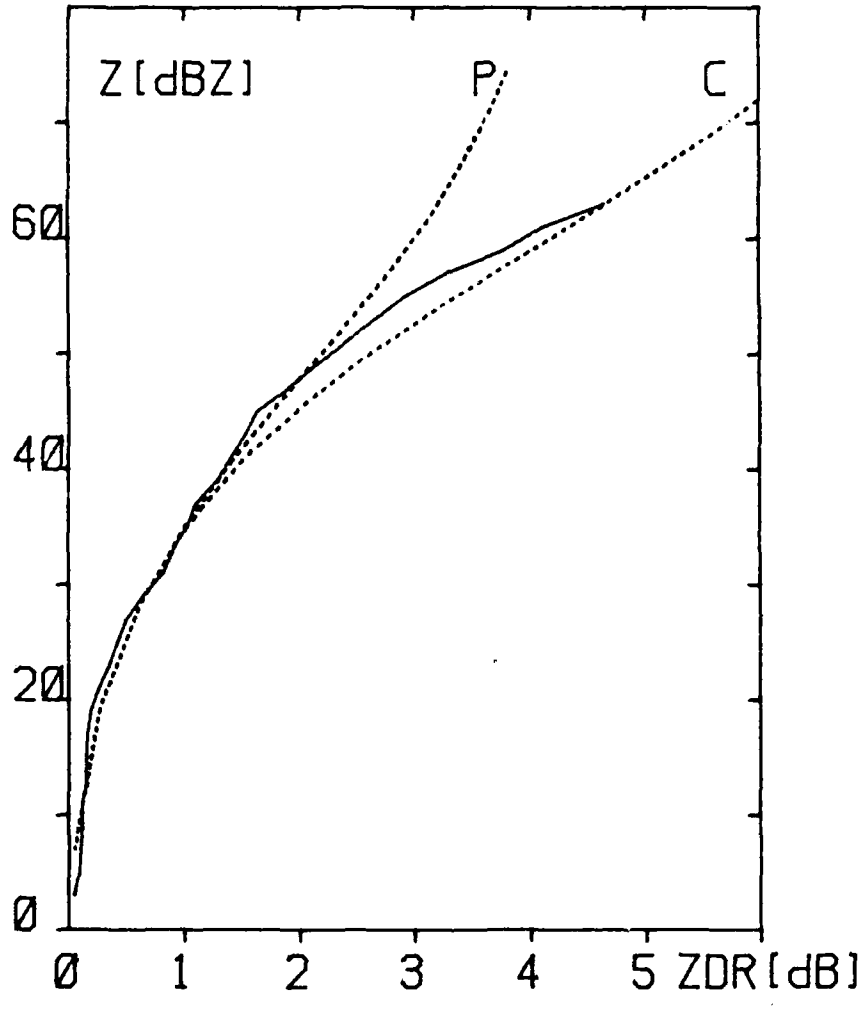

For explanation see Text, Section 3.

APPENDIX A

Reprinted from Nature, Vol. 320, No. 6061, pp. 431-433, 3 April 1986

Detection of hail by dual-polarization radar

A. J. Illingworth*, J. W. F. Goddard† & S. M. Cherry†

* Department of Physics, University of Manchester Institute of Science and Technology, PO Box 88, Manchester M60 1QD, UK
† Rutherford Appleton Laboratories, Chilton, Oxfordshire OX11 0QX, UK

Hail causes considerable damage to property and agriculture and a simple, unambiguous method of determining which convective storms contain hail would be of great use for short-term weather forecasting, and would also find application in the study of the mechanism of hailstone growth. Previous radar methods of hail detection[1-3] have not proved reliable, but here we report results of a new technique based on the measurement of differential reflectivity using dual polarization radar and suggest an additional criterion for hail recognition. Hail is known to occur in vigorous convective storms in which the effective radar reflectivity, Z, measured by conventional radar is high. If the hail reaches the ground it is usually restricted to long narrow swathes[4], often about 1 km wide but up to 50 km long, accompanied by surrounding precipitation in the form of heavy rain. The differential reflectivity technique involves comparing the radar reflectivity factor for horizontally (Z_H) and vertically (Z_V) polarized radiation; the comparison provides a measure of the mean shape of the precipitation particles. Close to the ground the values of Z are high for both hail and heavy rain, but because the large raindrops are oblate and fall with their horizontal diameter greater than the vertical, the value of Z_H in the rain exceeds that of Z_V. The smaller regions where hail is present can be clearly distinguished from the neighbouring heavy rain because, although individual hailstones may not be spherical, they tumble as they fall and so result in equal values of Z_H and Z_V.

For meteorological radars the power scattered back by common precipitation particles is proportional to the sixth power of the particle size and, although the particles may be frozen or liquid and may be non-spherical, it is usual to express the return as the equivalent radar reflectivity factor, Z, defined as the summation per unit volume of the diameter, raised to the sixth power, of spherical water drops which would scatter the same power as that actually measured. Z is usually quoted in decibels above 1 $mm^6 m^{-3}$. A full review of meteorological applications of radar is provided by Browning[5].

The new method of hail detection relies on a measurement of the differential reflectivity, Z_{DR}, defined in decibels as

$$Z_{DR} = 10 \log_{10} (Z_H / Z_V)$$

The radar used in this study is fully described by Cherry and Goddard[6]. Situated at Chilbolton in southern England, it has an antenna of 25 m diameter, giving a 0.25° beamwidth at the 10 cm operating wavelength. Pulses with horizontal and vertical polarizations are transmitted (and received) alternately with a pulse repetition frequency (PRF) of 610 Hz. The precipitation forms an incoherent target with the values of Z fluctuating as the hydrometeors reshuffle in space, but this choice of PRF ensures adequate correlation of Z between sequential samples so that Z_{DR} may be estimated accurately. Each range-gated data sample comprises a spatial average over 300 m (four pulse volumes), which is time averaged over 64 transmitted pulse pairs. The worst case errors in measuring Z and Z_{DR} are estimated to be 0.7 dBZ and 0.2 dB respectively.

A vertical section through a vigorous convective storm is

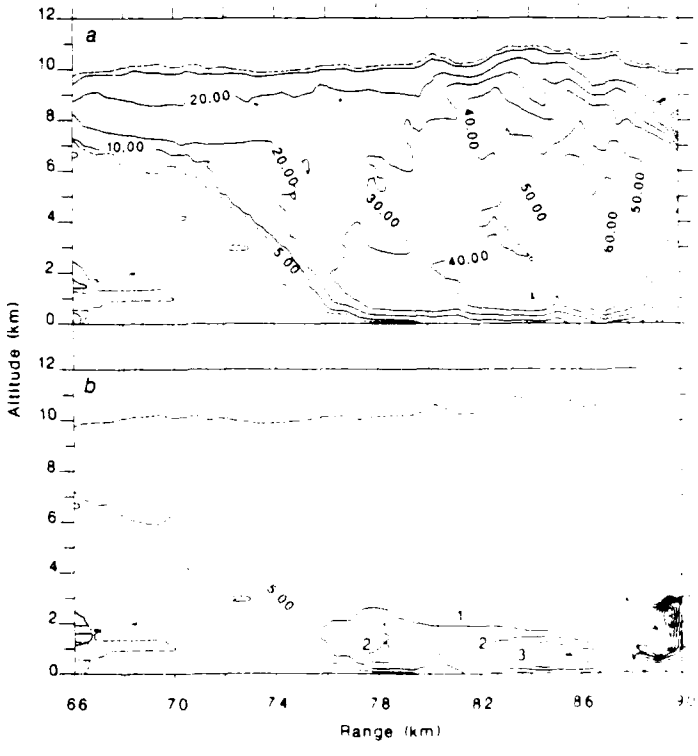

Fig. 1 Contour plots of reflectivity Z (*a*) and differential reflectivity Z_{DR} (*b*) obtained from a vertical scan through an intense convective storm at 13:36 UT, 6 July 1983. *a*, Contours of Z are drawn every 10 dBZ above 1 $mm^6 m^{-3}$, with an additional dotted 5-dBZ contour. *b*, Contours of Z_{DR} are plotted at 1-dB intervals starting at 1 dB. The dotted 5-dBZ contour from *a* is included, to delineate the extent of the echo. The positive values of Z_{DR} below 2 km altitude are due to raindrops falling with their horizontal axis larger than the vertical. In contrast to this is a narrow region at 87 km (<1 km wide) at 87 km range where near-zero values of Z_{DR} extend down to the ground. We believe that this region contains tumbling hail falling to the ground

shown in Fig. 1. In Fig. 1*a*, contours of the conventional reflectivity Z are drawn every 10 dBZ, from 10 dBZ to 70 dBZ above 1 mm^6 m^{-3}. In Fig. 1*b*, contours of Z_{DR}, observed simultaneously, are drawn at 1-dB intervals. The dotted Z contour at 5 dBZ in *a* and *b* delineates the overall extent of the echo. On this day the 0 °C isotherm was at about 3 km altitude, and (as is typical for convective clouds[7]) values of Z_{DR} at higher altitudes in Fig. 1*b* are very close to zero, indicating randomly tumbling ice particles. Closer to the ground where it is warmer than 0 °C, rain is to be expected, and as the rain intensity increases the drops become larger and more oblate, leading to larger values of Z_{DR}; assuming a Marshall–Palmer raindrop size distribution[8], calculations show[9] that Z_{DR} should exceed 1 dB when the Z value exceeds 35 dBZ. In contrast to this is a region at a range of about 87 km where low values of Z_{DR} extend down to the ground. For a width of about 600 m (that is, over two neighbouring samples), a Z_{DR} below 0.5 dB accompanied by a Z of 65 dBZ extends down to a radar elevation of zero degrees. For monodispersed raindrops this value of Z_{DR} implies diameters less than 2 mm, which would need to be present in the unrealistic concentration of 500,000 m^{-3} to give the observed Z. This corresponds to rainfall rates of thousands of millimetres per hour, and any other distribution would require even higher concentrations. The only plausible explanation is that the precipitation is hail which is nearly spherical or tumbles as it falls. The hail must be large, and with a high terminal velocity, so that although the surface is wet it has not melted sufficiently to form an oblate-shaped water coating. A similar but less extreme case can be seen in Hall *et al.*[7]

To monitor hail over a large area, the radar could be scanned in azimuth at low elevation so that in the summer only precipitation at temperatures much above 0 °C is sampled. If regions where Z is above 45 dBZ are considered, then any region where Z_{DR} is less than 0.7 dB can be identified as hail reaching the ground. Hail-swaths could be tracked by monitoring the movement, in successive scans, of such low-Z_{DR} cores embedded in regions of both high Z and Z_{DR}.

The technique outlined above would not result in false alarms. However, the precise shape and fall-mode of hail is not well known and if aspherical hail falls with a degree of common alignment, then Z_{DR} might have a local minimum but not fall below the 0.7 dB level. In 1986 the Chilbolton radar will be able to detect the orthogonal return in addition to the co-planar one. This information may provide additional corroborating evidence for hail. The linear depolarization ratio, L_{DR}, for vertically polarized transmitted radiation is defined as

$$L_{DR} = 10 \log_{10} (Z_{V,H}/Z_{V})$$

where $Z_{V,H}$ is the horizontally polarized return. L_{DR} values of less than −20 dB have been measured[10] in rain at a 3.2-cm wavelength. The orthogonal return is very low in amplitude because it is believed[11] that raindrops fall with their axes aligned in the vertical, with canting angles of less than 1°. Hail is generally aspherical and computations[12] show that randomly tumbling wet oblate spheroids with an axial ratio of 0.7 should have an L_{DR} greater than −20 dB. If this is so, the L_{DR} hail signature is simple: summertime values of L_{DR} above −20 dB close to the ground must be due to hail. The extreme case of spherical hail would escape L_{DR}-detection, but would give a clear zero Z_{DR} signal. At present there are no reports of measurements of L_{DR} at a 10-cm wavelength, but analysis of data at 3 cm (supplied by P. H. Herzegh, personal communication) confirms that, although propagation problems affect the absolute values of L_{DR}, a local increase of about 6 dB appears to coincide with a hail shaft.

The presence of hail seems to be the only physically realistic explanation of the localized region of low Z_{DR} embedded in a more extensive region where both Z and Z_{DR} are high. Although it has not been possible to obtain independent ground-based observations in the 500-m-wide region shown in Fig. 1, a long series of comparisons[13] of the radar data with simultaneous raindrop size distributions measured at the ground reveals that such high Z–low Z_{DR} combinations are not found in rainfall. More extensive observations with the Chilbolton radar scanning in azimuth at low elevation should enable the tracking of low-Z_{DR} cores and any accompanying anomalous-L_{DR} regions, and thus increase the probability of obtaining independent ground-based confirmation of the hail identification.

We acknowledge support from the Meteorological Office and EOARD through grant AFOSR-85-0188. We thank R. E. Carbone, P. H. Herzegh, V. N. Bringi and T. A. Seliga for supplying us with L_{DR} data from the Maypole '84 program.

Received 11 November 1985; accepted 12 February 1986.

1. Geotis, S. G. *J. appl. Met.* **2**, 277–284 (1963).
2. Carbone, R. E. *et al. Bull. Am. met. Soc.* **54**, 921–925 (1973).
3. Barge, B. L. *McGill Univ. Sci. Rep. MW-71*, Montreal (1972).
4. Morgan, G. M. & Towery, N. G. *J. appl. Met.* **14**, 781–786 (1975).
5. Browning, K. A. *Rep. Prog. Phys.* **41**, 761–806 (1978).
6. Cherry, S. M. & Goddard, J. W. F. *IEE Conf.* Bournemouth, pp. 54–58, IEE (1982).
7. Hall, M. P. M., Goddard, J. W. F. & Cherry, S. M. *Radio Sci.* **19**, 132–140 (1984).
8. Marshall, J. S. & Palmer, W. *J. Met.* **5**, 165–166 (1948).
9. Illingworth, A. J., Goddard, J. W. F. & Cherry, S. M. *Am. met. Soc. 22nd Radar Met. Conf.*, Boston, 145–150, American Meteorological Society (1984).
10. Browne, I. C. & Robinson, N. P. *Nature* **178**, 1078–1079 (1952).
11. Beard, K. V. & Jameson, A. R. *J. atmos. Sci.* **40**, 448–454 (1983).
12. Atlas, D., Kerker, M. & Hitschfeld, W. *J. atmos. terr. Phys.* **3**, 108–119 (1953).
13. Goddard, J. W. F. & Cherry, S. M. *Am. met. Soc. 22nd Radar Met. Conf.*, Boston, 342–347, American Meteorological Society (1984).

Printed in Great Britain by Macmillan Production Ltd, Basingstoke, Hampshire.

23rd Conference on Radar Meteorology, Snowmass, Boulder Colorado.
September 1986

OBSERVATIONS OF THE GROWTH AND EVOLUTION OF RAINDROPS USING DUAL-POLARIZATION RADAR

I J Caylor and A J Illingworth

Dept of Physics, UMIST, Manchester M60 1QD, UK

1. INTRODUCTION

As raindrops grow in size they become more oblate and consequently the radar reflectivity factor for horizontally polarised radiation (ZH) becomes increasingly larger than that for the vertical. The differential reflectivity, ZDR, expressed in decibels is defined as

$$ZDR = 10 \log (ZH/ZV)$$

ZDR is positive for rain and its magnitude provides an estimate of the mean size of the raindrops. Because ZDR is independent of concentration, observations of Z and ZDR can be fitted to any two parameter raindrop size distribution and used to derive more accurate rainfall rates than those obtained from Z alone (Seliga and Bringi, 1976, Goddard and Cherry, 1984).

The Chilbolton radar, situated in Hampshire England, operates at 9.75 cm with a quarter degree beamwidth and is able to measure Z to within 0.7dB and in widespread precipitation ZDR of 0.1dB (Cherry and Goddard, 1982). If we consider raindrops as oblate spheroids and apply Gans' scattering theory, then a change of ZDR of 0.1dB is equivalent to a change in axial ratio of less than 0.01. The best currently available laboratory measurements of equilibrium raindrop shapes (Pruppacher and Pitter, 1971) have errors in axial ratio considerably greater than 0.01. In a series of comparisons of radar observations for values of ZDR up to 2dB, with both ground based disdrometers (Goddard et al, 1983) and airborne measurements (Cherry et al, 1984) found significantly improved agreement if they used slightly more spherical shapes than those of Pruppacher and Pitter. The changes proposed by Goddard and Cherry are actually within the experimental error of the Pruppacher and Pitter measurements.

A ZDR value of 2dB is equivalent to a mean drop size of about 1.7mm, and average rainfall rates of about 40mm/hr. In this paper we analyse the values of ZDR for heavier rainfall rates and, so that consistency may be preserved with the radar results, suggest an empirical modification to the Pruppacher and Pitter shapes for the larger drops. In the light of these modifications, we then interpret some observations of the evolution of ZDR within vigorous convective clouds in terms of the size and concentrations of raindrops. We have payed particular attention to the narrow columns of positive ZDR which occasionally extend above the zero degree isotherm during vigorous convection.

2. THE SHAPE OF LARGE RAINDROPS.

Doviak and Zrnic (1984) have calculated that ZDR values above 3.5dB imply targets other than raindrops and suggest that they result from ice particles which have very oblate shapes when they melt. This assertion is based on Green's (1975) formula for the axial ratio of raindrops, which is very close to the measurements of Pruppacher and Pitter. Using these shapes a 6mm drop would be associated with a ZDR of 3.8dB and an 8mm drop 4.7dB; summing the weighted contributions of the various drops in a Marshall-Palmer raindrop size distribution leads to the conclusion that the ZDR of rain cannot exceed 3.8dB.

Values of ZDR above 3.5dB and as high as 6dB have been reported in convective showers (Illingworth et al, 1984) and in view of the above argument it seems logical to attribute such observations to melting ice particles. On closer examination other possibilities arise. First, recent laboratory measurements of melting particles suggest that unless the ice particles are initially extremely oblate then the shapes during melting are no more distorted than those of the same sized raindrop, and second, there are considerable experimental errors in the Pruppacher and Pitter shapes for the larger drops.

The laboratory studies of Rasmussen et al (1984) show that as spherical hail particles melt they become progressively more oblate until, on complete melting, their axial ratio is equal to that of the equivalent water drop. Hail pellets larger than 9mm always shed the excess water. A ZDR of 6dB could result from horizontally aligned ice particles with a wet surface and an axial ratio of 0.52. This seems unlikely because such large solid particles should tumble, and hail is rarely observed to have such an oblate shape. High values of ZDR attributed to melting snowflakes (Hall et al, 1984) would only occur in stratiform clouds and should be restricted to the bright band.

There is considerable uncertainty as to the precise shape of raindrops above 4mm diameter. Laboratory experiments are difficult because the drops oscillate, and the degree of oscillation is probably dependent upon the amount of turbulence in the wind tunnel. Pruppacher and Pitter quote equilibrium axial ratios for drops of 6 and 8mm diameter which would lead to ZDR values of 3.8 and 4.7dB respectively, but, because of the experimental errors quoted, these axial

APPENDIX B

ratios could be as low as 0.62 and 0.51, implying a ZDR of 4.7 and 6.5dB. It is difficult to check these predictions in the field. Direct aircraft measurements by Cooper et al (1983) showed that for a given equivalent diameter there was a spread of axial ratios implying appreciable oscillation, but that the mean shape for 5mm drops was significantly more distorted than Pruppacher and Pitter's measurements. Only a very few drops above 6mm were sampled but they indicated an axial ratio of only 0.5 for a 6.5mm drop.

If the concentration of raindrops, N, of diameter D, is assumed to follow the Marshall-Palmer raindrop distribution

$$N(D) = No \exp(-3.67\, Do/D)$$

where No is 8000/m3/mm, then if the drop shapes are known we can calculate ZDR as a function of Z. Figure 1 compares the predicted variation using the Pruppacher and Pitter shapes and an extrapolation of the more oblate measurements of Cooper et al. The actual values of axial ratio used in these computations are displayed in Table 1. It should be stressed that Cooper et al did not measure any drops above 7mm, and that the axial ratios for drops above this size are obtained by linear extrapolation. The dotted curves in Figure 1 were obtained by truncating the exponential distribution at 8mm; observation shows an insignificant number of drops larger than this size. Such a truncation can be introduced more naturally by using a gamma distribution (Ulbrich, 1983), and the dashed branches of the curves are the predicted variations for an m of 2 in the gamma distribution. The solid branch of the curves is obtained by truncating a pure exponential (m = 0) at 7mm. These variations introduced by different choices of drop size distribution are small compared with the effect of the two different models for the drop shapes. If the more oblate shapes are adopted then it appears that values of ZDR of up to 6dB can arise in heavy rain.

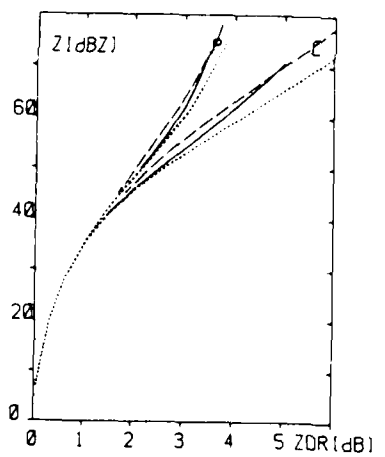

Fig 1: Theoretical relationship between Z and ZDR for various drop size distributions using shapes from Pruppacher and Pitter (P) and extrapolated from Cooper et al (C).
..... Marshall-Palmer truncated at 8mm
——— Marshall-Palmer " 7mm
-------- Gamma function m=2 " 8mm

3. RADAR DERIVED SHAPES OF LARGE DROPS.

We have indicated above that independent verification of the predicated Z/ZDR relationship by direct measurement of the raindrops within the radar beam is not practically possible. Instead we have adopted a statistical approach; although on individual occasions the drop size distributions are not Marshall-Palmer, if sufficient data points are taken then the average variation of Z as a function of ZDR should provide an indication of the drop shapes. Over ninety thousand data points from storms observed on six different days in 1983 are included in the plot displayed in Figure 2, where the average values of ZDR have been calculated for every 2dB increase in Z. For comparison purposes the theoretical curves from Figure 1 for the two different sets of drops shapes predicted for exponentials truncated at 8mm are also included. On these days the freezing level was at 3km and all data points for altitudes between 0.25 and 1km were analysed. At such low altitudes most of the

D	Pruppacher and Pitter (1971)		Cooper et al (1983)	
(mm)	b/a	ZDR (dB)	b/a	ZDR (dB)
4	.77	2.59	.77	2.59
4.5	.74	2.98	.71	3.38
5	.716	3.30	.65	4.23
5.5	.697	3.56	.6	5.00
6	.679	3.81	.55	5.82
6.5	.664	4.03	.50	6.72
7	.654	4.18	.45	7.70
7.5	.641	4.31	.40	8.78
8	.619	4.70	.35	9.99

Table 1: The axial ratio (b/a) and differential reflectivity (ZDR) for raindrops having equivalent diameter (D) of 4 to 8mm using the drop shapes of Pruppacher and Pitter (1971) and values extrapolated from Cooper et al (1983).

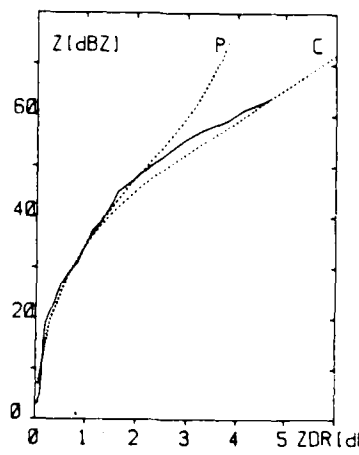

Fig 2: Solid curve: The average value of ZDR for every 2dB interval in Z. 90,000 data points at altitudes between 0.25 and 1km.
Dotted lines: curves from Fig 1 for a Marshall Palmer drops size distribution truncated at 8mm.

precipitation should be rain, but on a few scans the Z/ZDR plots showed a fall in ZDR for values of Z above 50dBZ. Figure 3 shows an example of this. We believe (Illingworth *et al*, 1986) that this behaviour is due to large tumbling hail particles surviving the 2km fall below the freezing level. Figure 4 is a contour plot of a PPI, clearly showing the core of ZDR below 0.5dB occuring at the centre of the maximum Z echo, which we interpret as a hail shaft. The occasional section showing such characteristics was excluded from the analysis. The standard deviation of the points in Figure 2 for ZDR above 2dB is about 0.7 dB in ZDR, showing that on the average each individual size distributions does not have a value No = 8000.

The observed variation of ZDR with Z in natural rain shown in Figure 2 deviates significantly from the predictions of the Pruppacher and Pitter shapes, and is very close to the values computed using the much more oblate shapes extrapolated from Cooper et al. An alternative explanation would be to consider that the Pruppacher and Pitter shapes are valid, but, that when Z is high, No falls below 8000/m^3/mm. For example a ZDR of 3.6dB should on average be accompanied by a Z of 70dBZ if No is 8000/m^3/mm. In fact the average value is only 58dBZ implying that, for this high value of Z, No is less than 800, and that the rainfall rate is correspondingly lower than that which would occur for No = 8000. This seems unlikely. Calculated rainfall rates using No = 8000 agree with the empirical Z/R relationships to within 1dB. If we use the more oblate raindrop shapes in the model then the empirical Z/R relationship is not disturbed, the observed variation of Z with ZDR can be explained, and furthermore the high values of ZDR of 6dB can be attributed to raindrops without invoking extraordinary oblate aligned melting ice particles.

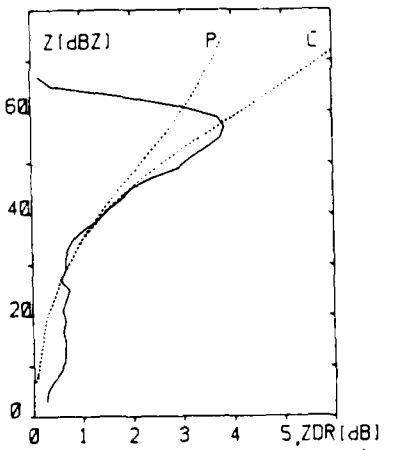

Fig 3: Solid line: The variation of Z with ZDR in one PPI. Such data is attributed to hail and is not included in Fig 2. Dotted lines as in Fig 2.

4. EVOLUTION OF RAINDROPS.

In convective clouds the value of ZDR above the 0°C isotherm is observed to be very close to zero with values generally below 0.1dB, and this is interpreted as tumbling graupel. On occasion localised areas of positive ZDR extend above the freezing level (Illingworth et al, 1984) and these are generally in the form of narrow columns as shown in Figure 5.

During the summer of 1983 twenty columns of +ve ZDR having values of ZDR above 2dB were observed. In ten of these cases it was possible to trace the evolution of the column from three or more sequential RHIs taken at the same azimuth, each RHI at the same azimuth being typically separated by about two minutes. These cases occured in both isolated initial echoes and embedded within mature cumulonimubs clouds. Considering the individual RHIs, we conclude that the positive columns of ZDR have the following characteristics:

a) *The maximum height of the 2dB ZDR contour was* 1.7 km above the zero degree isotherm where the temperature was about -10°C. Just above this height and in the region surronding the column ZDR values are less that 0.1dB.

b) Well-developed columns rising more than 700m *above the freezing level have a circular* cross-section with a diameter between 1 and 2km.

c) For such columns the maximum value of ZDR exceeds 4.5dB and can reach 6dB; a further 500m higher, values of ZDR are zero.

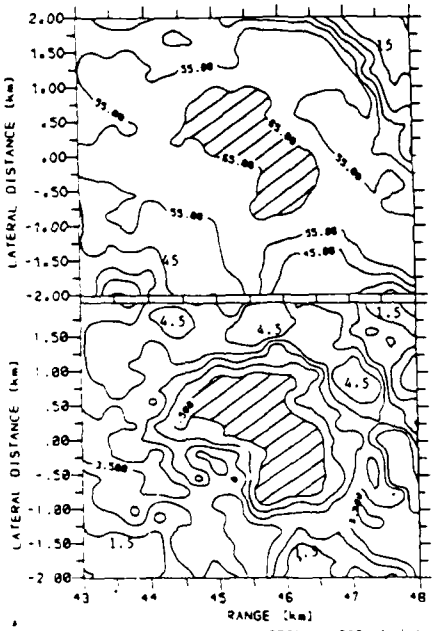

Fig 4: A horizontal section (PPI) at 900m height observed at 1517 on 6/Jul/83. The hatched area where Z is below 0.5dB and Z is above 65dBZ is attributed to hail. Contours in ZDR are every 1dB starting at 0.5dB and in Z are every 10dB.

From the sequential RHIs we conclude:

d) A well defined positive column does not persist for more than ten minutes.

e) While the positive column is present the magnitude of Z increases by up to 20dBZ, finally exceeding 58dBZ. In one case however the value of Z only rose from 38 to 46dBZ.

f) During the development of the positive column the +2dB ZDR contour rises at about 7m/s; this rise being coincident with a similar rate of ascent for either the 20dBZ contour in Z for the isolated developing cells, or the 40dBZ contour for the columns embedded in existing cells. These figures imply that the air itself is rising at about 15m/s.

g) Interpreting the Z and ZDR data in the column as the size and concentration of supercooled raindrops, the derived values of No always tended to increase with time towards the Marshall-Palmer value of 8000. For isolated convection this increase in 6 minutes was about a factor of 50, and for the embedded convection a factor of two in two minutes. In the one case (see (e)) No remained near 200.

h) After the disappearance of the positive ZDR column, the position of the maxima in both Z and ZDR fell in altitude at a velocity consistent with the terminal velocity of the large precipitation particles.

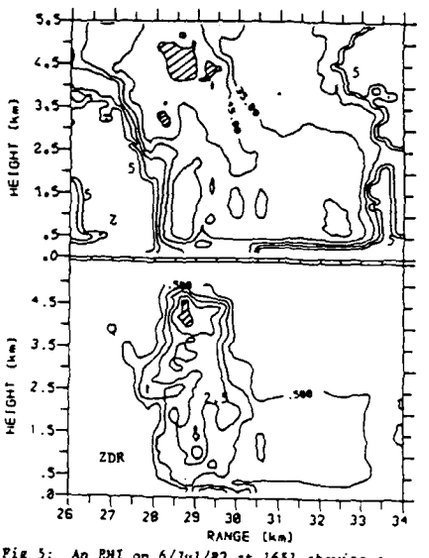

Fig 5: An RHI on 6/Jul/83 at 1651 showing a column of +ve ZDR reaching a height of 4.7km. 0°C isotherm 3.2km. Contours in Z every 10dBZ starting at 5dBZ, and in ZDP every 1.0dB starting at 0.5dB. Hatched area Z above 55dBZ, ZDR above 4.5dB.

5. CONCLUSIONS

The observed values of Z and ZDR in heavy precipitation are consistent with the more oblate shapes reported by Cooper et al. We suggest that positive values of ZDR of up to 6dB are due to large raindrops which may be supercooled, and that hail or graupel particles which are wet will have smaller values of ZDR than the equivalently sized raindrop. Transient positive columns of ZDR extending up to 1.7km above the freezing level occur during vigorous convection; initially, raindrop concentrations are low but they evolve towards the Marshall-Palmer distribution.

6. ACKNOWLEDGEMENTS.

We are grateful to J W F Goddard and S M Cherry for making the radar measurements and for many helpful discussions. This research was supported by the Meteorological Office, by NERC grant, GR3/5896 and by AFOSR-85-0188. Computing facilities were provided by SERC under GR/D 69372.

7. REFERENCES

Cherry, S. M., and Goddard, J. W. F., 1982, Design features of dual-polarisation radar URSI Conference, Bournemouth, United Kingdom.

Cherry, S. M., Goddard, J. W. F., and Guldridge, M., 1984, Simultaneous measurements of rain by airborne distrometer and dual-polarisation radar. Radio Sci, 19 169-176.

Cooper, W. A., Bringi, V. N., Chandrasekhar, V., and Seliga, T. A., 1983, Analysis of raindrop parameters using a 2-D precipitation probe with application to differential reflectivity. 21 Conf on Radar Meteorol, AMS, Boston.

Doviak, R. J., and Zrnic, D. S., 1984, Doppler Radar and Weather Observation, Academic Press, Orlando, Florida.

Goddard, J. W. F., Cherry, S. M., and Bringi, V. N., 1983, Comparisons of dual-polarisation radar measurements of rain with ground-based distrometer measurements. J. App. Met., 21 252-256.

Green, A. W., 1975, An approximation for the shape of large raindrops. J. App. Met., 14 1578-1583.

Hall, M. P. M., Goddard, J. W. F., and Cherry, S. M., 1984, Identification of hydrometers and other targets by dual-polarisation radar. Radio Sci, 19 132-140.

Illingworth, A. J., Goddard, J. W. F., and Cherry, S. M., 1984, Dual linear polarisation studies of the evolution of convective storms. 22nd Conf. on Radar Meterol. AMS, Boston.

Illingworth, A. J., Goddard, J. W. F. and Cherry, S. M., 1986, Detection of hail by dual-polarisation radar. Nature, 320 431-433.

Pruppacher, H. R., and Pitter, R. L., 1971, A semi-empirical determination of the shape of cloud and rain drops. J. Atmos. Sci. 28 86-94.

Rasmussen, R. M., Levizzani, V., and Pruppacher, H. R., 1984, A wind tunnel and theoretical study of the melting behaviour of atmospheric ice particles: III Experiment and theory for spherical ice particles of radius 500 m. J. Atmos. Sci. 41, 381-388.

Seliga, T. A., and Bringi, V. N., 1976, Potential use of radar differential reflectivity measurements at orthogonal polarisation for measuring precipitation. J. App. Met 15 69-76.

Ulbrich, C. W., 1983, Natural variations in the analytical form of the raindrop size distribution. J. Clim. & Appl. Met, 22 1764-1775.

POLARISATION RADAR STUDIES OF PRECIPITATION DEVELOPMENT IN CONVECTIVE STORMS

A J Illingworth*, J W F Goddard+ and S M Cherry+

*Department of Physics, UMIST, Manchester M60 1QD

+Rutherford Appleton Laboratories, Chilton, Oxon OX11 0QX

June 1986

APPENDIX C

1 INTRODUCTION

Our present knowledge of how precipitation develops within clouds has been obtained using both radar and instrumented aircraft. Measurements of the radar reflectivity, Z, provide an indication of the rainfall rate; air motions can be computed from multiple doppler radar, and hydrometeor types and sizes may be obtained from probes mounted on aircraft. However, information on hydrometeors is generally available only for a very limited number of one dimensional penetrations through the less vigorous regions of a cloud, and a complete history of the hydrometeor evolution throughout the volume of the cloud can only be built up by extrapolation from these limited samples (e.g. Hallett et al, 1978; Knight and Squires, 1982; Heymsfield and Hjelmfelt, 1984, and for hail growth, Browning et al, 1976, Browning 1978).

Several radar scans through a cloud do provide a reasonably complete three dimensional picture of the extent and intensity of the radar reflectivity, Z, but Z itself gives no information on hydrometeor types, sizes or concentrations. Several empirical relationships are available which relate Z to the rainfall rate R, but because Z is proportional to the product ND^6 summed over particles of all sizes (where N is the concentration of hydrometeors of diameter D), the use of such Z-R relationships is error prone and is equivalent to assuming that all hydrometeor size distributions are identical. The same Z could result from many different size distributions having widely varying equivalent rainfall rates. An additional ambiguity occurs if mixed phase clouds are present, because liquid water has a reflectivity 6.7dB greater than ice; for melting particles interpretation of Z is even more error prone.

In this paper we present measurements not only of Z but of the differential radar reflectivity, Z_{DR}, of evolving convective clouds. This additional parameter can reduce considerably the ambiguities present in the interpretation of Z alone.

measurement. Each range-gate data sample comprises a spatial average (linear power) over 300m (four pulse volumes). At 60km the sample volume is typically a cube of side 300m in length. Time averaging (linear power) for each data sample is over 210ms every 240ms (i.e. 64 transmitted pulses on each polarisation). The worst case systematic errors in measuring Z and Z_{DR} were estimated to be 0.7dB and 0.1dB, respectively, while the standard deviations of the random errors when measuring rain echoes were estimated to have the same values. A detailed study of the accuracy of the measurement has been given by Cherry and Goddard (1982).

Herzegh and Carbone (1984) have shown that when strong reflectivity gradients in Z are present, a mismatch of the polarisation characteristics of the antenna sidelobes may give rise to totally false Z_{DR} values. In this case it is possible for the main beam to be sensing a low reflectivity region, but for a significant part of the reflected signal to be due to the sidelobe detecting the high Z region. They give examples from the 1° beamwidth CP2 radar where mismatched sidelobes result in spurious regions of high positive and negative Z_{DR} on either side of a reflectivity maximum. Very much higher reflectivity gradients would be required to produce such effects for the quarter degree beamwidth of the Chilbolton radar, but we shall return to this potential problem when discussing the observations in Section 3.

(b) Z_{DR} of Rain

If hydrometeors are assumed to be oblate spheroids, having their figure axes vertical, then application of Rayleigh scattering theory gives the curves in Figure 1 (from Hall et al, 1984) showing the value of Z_{DR} as a function of axial ratio for liquid water and air-ice mixtures. The Figure clearly demonstrates that for a given shape this ratio is much larger for liquid water than for ice. For rain it is probably valid to assume that the drops fall with their figure axes aligned in the vertical, but any canting or tumbling will lead to lower values of Z_{DR}: in the extreme case of random tumbling, which may occur for ice particles, Z_{DR} will be zero.

The most accurate laboratory measurement of equilibrium raindrop shapes is provided by Pruppacher and Pitter (1971). In a series of comparisons of radar observations for values of Z_{DR} up to 2dB, with both groundbased distrometers (Goddard et al, 1983) and airborne measurements (Cherry et al, 1984) Goddard and Cherry (1984a) found significantly improved agreement if they used slightly more spherical shapes than those of Pruppacher and Pitter. This modified relationship between drop diameter and Z_{DR} is displayed on the abscissa of Figure 2. Oscillations of raindrops are believed to be asymmetric, and if these are excited then a time averaged shape should be more spherical than the equilibrium one, and this could reduce the observed value of Z_{DR} (Beard et al, 1983). It could be argued that because oscillations are collision induced, any correction to Z_{DR} would have to be concentration dependent. Direct photography of raindrops at the ground (Jones, 1959) indicates that a degree of canting is present, but the wind shear at the ground may not be representative of conditions within clouds; computations (Beard and Johnson, 1983) suggest that shear produced by turbulence would lead to small canting angles distributed around a mean zero value. However, the changes proposed by Goddard and Cherry are actually within the experimental error of the Pruppacher and Pitter measurements, and so there is no evidence that canting or collision induced oscillations affect the Z_{DR} measurement of rain. The calibration of Z_{DR} is so sensitive to drop shape that at present it is able to detect changes in shape that cannot be resolved by direct photography.

If both Z and Z_{DR} are measured for rain then the data can be fitted to any two parameter raindrop distribution. Figure 2 considers one extreme example, the monodispersed spectrum, and for a given Z_{DR} the curves show the expected values of Z for a rainfall rate of 1mm hr^{-1} and for drop concentrations of 1 and 100 per cubic meter. Because Z_{DR} is independent of concentration, the values of N and R scale linearly with Z. There is uncertainty over the average shape of drops having an equivalent diameter above 4mm. Some recent aircraft measurements (Cooper et al, 1983) suggest that they are more oblate than the equilibrium shapes of Pruppacher and Pitter, with a 6mm drop having a Z_{DR} of 5.8dB instead of 3.8dB,

and an indication that the values of 7mm drops should be 7.7dB rather than 4.18dB. The two dotted branch to the curves in Figure 2 for Z_{DR} above 2.5dB are computed using these more oblate shapes.

The Marshall Palmer raindrop size distribution is given by

$$N(D) = N_o \, (\exp(-3.67 \, D/D_o)) \tag{2}$$

where N_o is $8000 m^{-3}$ mm^{-1} and constant, and D_o depends upon the rain rate and is equivalent to a median drop size such that an equal volume is contained in drops smaller and larger than D_o. If both Z and Z_{DR} are available then a fit to a generalised exponential distribution with both N_o and D_o as variables is possible (Seliga and Bringi, 1976). In Figure 3 the abscissa shows the relationship between Z_{DR} and D_o obtained by weighting the Z-D dependence in Figure 2 and truncating the exponential spectra at 8mm diameter. As above, because they scale linearly with Z, the values of N_o and R may be obtained by linear extrapolation of the plotted curves. According to this Figure values of Z_{DR} above 5dB cannot be fitted to realistic exponential raindrop size distributions if the drop shapes of Pruppacher and Pitter are used.

Some caution should be exercised in interpreting these curves for Z_{DR} values above 3dB because of the uncertainty in the precise shapes of the larger drops and the sensitivity of the curves to the truncation of the exponential. If the exponential is not truncated at 8mm then, for D_o above 4mm, because the very few drops above 8mm are so distorted, their contribution determines Z_{DR}. Consequently in very intense rain the shape of the drops at the truncation limit of 8mm-fixes the maximum possible value of Z_{DR} to about 3.5dB for Pruppacher-Pitter shapes. If the more oblate shapes of Cooper et al are used then an 8mm truncation limit would lead to a maximum Z_{DR} of around 6dB.

The sensitivity of predicted values of Z_{DR} in very intense rain to the rather arbitrary choice of the truncation limit of the exponential is rather artificial; the observed concentrations of these very large drops are in fact smaller. Ulbrich and Atlas (1984) have suggested introducing this effect more naturally by the use of gamma distributions of the form:

$$N(D) = N_o D^m \exp(-(3.67 + m)\, D/D_o)) \qquad (3)$$

The third variable, m, is zero for a pure exponential and infinity for monodispersed spectra and is a measure of spectral width. Ulbrich and Altas (1984) suggested using m = 2, but Goddard and Cherry (1984b) obtained even better agreement with measured rainrates for a value of m = 5. The magnitudes of N, N_o and R calculated from Figures 2 and 3 (m = infinity and zero) represent limits, with the true value of the total drop concentration probably lying between these two extremes. We note that for an observed Z and Z_{DR} combination the choice of the monodispersed spectrum will result in predicted rainfall rates typically 3dB greater than for the exponential spectrum.

(c) **Measurements of Hydrometeors above the 0° isotherm**

The shape of an ice particle and its mode of fall is not a unique function of its size and so the analysis of the Z_{DR} signal is complicated. Hall et al (1984) consider the problem in detail, and Figure 1 taken from their paper, demonstrates some of the possible ambiguities. Even if the particles were all aligned with the major axis horizontal we see that Z_{DR} would depend not only on the particle shape but also on the density. If they are not perfectly aligned as they fall, then the value of Z_{DR} will be lower, falling to zero for random tumbling. Further complications and ambiguities would arise if the actual ice particle shapes were used rather than idealised oblate spheroids.

From experience with the Chilbolton data Z_{DR} is usually very close to zero in regions of convective clouds where the temperature is below zero, indicating nearly spherical or randomly orientated tumbling ice particles. In the next section we shall be considering transitory regions of high positive Z_{DR} above 4dB within convective clouds which extend both above and below the zero degree isotherm and occur where Z is moderate or high. We shall now consider the types of hydrometeor which could give rise to such signals.

(i) **Dry ice particles**

From Figure 1 snow cannot give a Z_{DR} above 1dB, but a Z_{DR} of +4dB can result from dry aligned oblate spheroids of ice having axial ratios of 0.15 for an ice-air mixture of density 0.5g cm^{-3} or spheroids of solid ice with a ratio of 0.4. For example, Hall et al (1984) found regions of high positive Z_{DR} in the upper regions of stratiform clouds where Z is low and suggested that these may be due to small ice crystals in the form of plates which fall with their larger dimension horizontally aligned. Direct aircraft observations (Bader et al, 1986) flying through such clouds in 1984 have confirmed this suggestion. However, such small particles can give only low values of Z and on melting would acquire a water coating and give much larger values of Z_{DR} just below the 0°C isotherm before subsequently collapsing to smaller raindrops. Hall et al (1984) do find regions of positive Z_{DR} in association with the bright band in Z which are obviously caused by melting particles, but for the observations we shall present there was no bright band and the positive Z_{DR} extended 2km above the zero degree isotherm.

The various habits of ice crystal growth can result in extremely oblate shapes but because of their size would be associated with low values of Z. Larger ice particles are formed by aggregation or riming and there is no evidence from aircraft measurement that they would have both such a degree of oblateness and also be aligned when they fall. Although the fall mode of larger

frozen hydrometeors and hailstones is not well known (Thwaites et al, 1977, Matson and Huggins, 1980), most evidence suggests that discs tumble when the Reynolds number exceeds 1000 (Pruppacher and Klett, 1980).

(ii) **Ice in wet growth**

Hail or graupel particles in wet growth will have a Z_{DR} of 4dB if the axial ratio is 0.65. This could happen in two ways; either sufficient water builds up on a spherical particle, or a surface layer of water on a quite asymmetric hail pellet stabilises it and stops it tumbling. The particles would probably shed any excess water, but if for the sake of argument, we extend the analysis of Bailey and Macklin (1968) to smaller particles with a fall velocity of $V = 1.43\ (D)^{0.8}$ where D is in mm and V in $m\ s^{-1}$ (Pruppacher and Klett, 1980), we find that if the surface is to be wet, then for diameters of 2, 4 and 10mm, a cloud liquid water content of 13, 7.3 and 3.2g m^{-3} respectively is required. Even higher values would be needed for a reasonable thickness of water to build up, and for rough particles with higher ventilation coefficients these values should be increased threefold. From sonde ascents made on the days in question the maximum adiabatic liquid water content at 0°C and -10°C cannot exceed 5g and 7g m^{-3}. We conclude that small graupel particles in wet growth require unrealistic liquid water contents and would also melt to give much smaller Z_{DR} below the freezing level. Computation (Mason, 1956) shows that for solid ice spheres to fall 2km below the freezing level without melting completely, the original diameter must be at least 4mm; for graupel of density 0.3g cm^{-3} the equivalent size is 8mm. However, interpretation of these signals in terms of hail of diameter greater than 5mm which is in wet growth cannot be ruled out.

(iii) **Supercooled raindrops**

A simpler explanation of such signals would be to assume they are due to large supercooled raindrops, a Z_{DR} > 4dB being equivalent to a diameter of about 6mm; and when analysing these results we shall adopt this approach. We shall return to consider the wet growth aspects in the discussion Section.

3 RESULTS OBTAINED IN 1983

The aim of the 1983 studies was to trace the development of isolated convective clouds. Typical echoes from these clouds have horizontal diameters of about 5km and about 5 vertical sections (RHIs) at different azimuths were sufficient to identify the maximum echo and its spatial extent. Each RHI takes about 30 seconds, so an observation at any particular azimuth was obtained every 2 or 3 minutes. Occasional horizontal sections (PPIs) served to confirm the isolated character of the storms. Hall et al (1980) reported that pillars of -veZ_{DR} extending higher than the 0°C isotherm were occasionally observed, and suggested that they were due to supercooled raindrops. One particular goal was to find out if these columns of large -veZ_{DR} were a common occurrence and to study their persistence. Because there is no area of preferred convection over Southern England the location of first echoes is difficult, but in these examples the problem was alleviated, because winds were very light leading to minimal advection of cells, and on 6 and 7 July a slight shear resulted in the development of sequences of daughter cells.

3 (a 7 July 1635 to 1655

On this day the 1200 hrs sonde ascent from Crawley, over to the east of Chilbolton, showed that a further rise in surface temperature of 2 or 3 degrees would be sufficient to lift the moist low level air to the condensation level of 1.1km, this air could then, in the absence of mixing, rise to the 250mb level. Winds throughout the troposphere were very light from between 250 and 270° and at no height exceeded 5 m s^{-1}. The freezing level was at 3.3km, with unmixed cloudy air perhaps 2° warmer. In the afternoon a few vigorous showers developed.

Two weak isolated echoes 30 and 40km East of Chilbolton are clearly visible in Figure 4 which is a 2° elevation PPI. A further ten kilometers distant at 50km range is a much more extensive row of vigorous cells having reflectivities above 50dBZ. This PPI shows that at an altitude of 1.4km an isolated echo at 40 km range and 5km lateral distance has areas where Z is 20 to 30dBZ accompanied by anomalously high ZDR values above 3dB. This combination is so far from the predictions of a Marshall-Palmer raindrop size distribution (see Figure 3) that 42 RHI and 3 PPI scans were made through this cell in 30 minutes in order to trace its evolution; each RHI being separated by only 1°, which is equivalent to a distance of 700m at this range. The isolated cell at 30km range and -6km lateral distance has Z values above 20dBZ but is not accompanied by any unexpectedly high values of Z_{DR}.

The first vertical section through the most intense part of this weak echo obtained at 1635-40, three minutes before the PPI, is displayed in Figure 5. A vertical profile of Z and ZDR at the gate where the maximum Z occurs is plotted in Figure 6. RHIs at neighbouring azimuths show lower Z values. These data

confirm that the cell had a Z which only locally reached 34dBZ whereas the value of ZDR widely exceeds 2dB with a maximum of 4.1dB where Z is less than 30dBZ. In Figure 5 the high Z_{DR} region extends in a narrow column almost to the ground. Half-melted ice particles might give such a large Z_{DR} but they would need to be large to survive such a fall without complete melting, and raindrops would need to have a diameter of about 5 or 6mm to assume such an oblate shape. In either case the low values of Z must imply that such large particles are present in very low concentrations.

This cell subsequently intensified rapidly, but because of the light westerly winds did not change azimuth appreciably and the range only increased by about 1km every 10 minutes or so. The actual 30dBZ echo in Figure 5 did not grow, but, perhaps not suprisingly in view of the large particles below the maximum echo, it fell to the ground in the following five minutes, as did the subsidiary 10dBZ echo at 37km range. Instead a local maximum in Z of 24dBZ at 2.5km altitude acccompanied by a Z_{DR} of over 3dB located 1.4km to the south (2^{o} in azimuth) increased rapidly in intensity and areal extent, so that by 1641-10 the vertical section in Figure 7 was observed with the development of a narrow vertical column of positive Z_{DR}. The vertical profile displayed in Figure 8 taken through the most intense part of this column confirms values of Z_{DR} of 4dB above the freezing level with Z reaching 38dB at 4.8km altitude. Two minutes later the vertical sections indicate little change in the column but show that the maximum height of the 20dBZ contour has risen by just over 1km, equivalent to a vertical velocity of almost 10m s^{-1} A typical RHI obtained a further five minutes later at 1648-10 is displayed in Figure 9 and shows a quite different character.

Although the cloud has grown further and at 3km height Z has reached 54dBZ, a traditional hail signature, the column of positive Z_{DR} has vanished. The vertical profile of Z and Z_{DR} plotted in Figure 10 highlights this transformation. the Z_{DR} signature is now typical of that commmonly observed in mature glaciated cumulonimbus clouds. Above the freezing level Z_{DR} is generally within 0.1dB of zero, this is usually interpreted as tumbling hail or graupel pellets. Below the zero degree isotherm Z_{DR} gradually increases from 0 to 5dB over a distance of 2km, consistent with the particles slowly melting to form large oblate raindrops near to the ground. Three minutes later Z values of 61dBZ were observed. The Z_{DR} gradient in Figure 10 should be contrasted with the very abrupt fall off in Z_{DR} above 5km in Figure 8, which is difficult to explain in terms of particles falling and melting. A more plausible interpretation is to consider the sharp change occurring at the boundary where a rising parcel of air containing supercooled raindrops penetrates upwards into the glaciated region of the cloud.

The evolution from the first RHI in Figure 5 to the mature cloud in Figure 9 took only 12 minutes with the echo top rising nearly 4km at an average velocity of 5 m s^{-1}. The two minute period when there was a column of positive Z_{DR} extending towards the -10°C isotherm appeared to coincide with the most vigorous growth with the Z echo rising at about 10m s^{-1}. It is interesting to note that the second isolated weak Z echo in the PPI of Figure 4 which is at a range of 30km and a lateral distance of -6km, which was not accompanied by any large positive Z_{DR}, failed to develop.

3(b) 6 July 1606 to 1615

The 1200 sonde ascent from Crawley indicated a similar

structure to that already described on the 7 July. The calculated freezing level was 3.2km and the winds again were less that 5 m s^{-1}, but from a direction between 170 and 180°. An isolated daughter cell was first detected in the 5° elevation PPI which is displayed in Figure 11. This cell is at 30km range and 7km lateral distance, at larger lateral distances no returns were detected, but at 2km lateral distance only 3km from the cell is the start of a long narrow band of intense echoes extending aout 50km to the south. No echo was detected at the position of the isolated cell in the 4° elevation PPI where the height of the beam at this range would be about 2km. Because the 5° elevation showed such anomalously high Z_{DR} values of 2.4dB accompanied by a Z echo of 25dBZ, a series of 25 RHI scans through the cell was made in the 12 minutes following the PPI. Each RHI was separated by 2°, equivalent at this range to a horizontal distance of 1km. As the southerly wind was so light, the echo was remained between azimuths 141 and 149 throughout this period, advecting by less than 1km in 20 minutes.

Fig 12 displays the contours in Z and Z_{DR} for the first RHI at 1607-00 through the most intense section of this daughter cell. The daughter cell has a maximum Z of 33dBZ but, as in the example of 7 July, is accompanied by much nigher values of Z_{DR} than would be predicted by most commonly observed raindrop size distributions. This is further demonstrated by the vertical profiles in Z and Z_{DR} in Figure 13, where values of Z_{DR} of 3dB are found where Z is only 30dBZ. By similar arguments to those employed in Section 3(a) these particles must be large raindrops or large melting ice particles and so the low Z value implies the particles are present in very low concentrations.

This daughter cell grew rapidly and the vertical section in

Figure 14 was obtained 6 minutes later at 1613-20 with the highest Z value of 51dBZ coinciding with the maximum observed Z_{DR} of 5.1dB. Again the Z_{DR} contours show a well developed narrow vertical column containing the highest values of differential reflectivity which extends over 1.5km above the freezing level to where the temperature is about -10°C. As this feature is virtually absent on the neighbouring RHIs we conclude that the diameter of the column is only about 1km. An RHI 2 minutes later still shows the Z_{DR} column, while Z has further increase to 61dBZ and the echo top has risen a further 1 km implying an upward velocity of close to 10 m s^{-1}.

The evolution is simpler than the previous example in that only one maximum in the echo could be distinguished, however by the time of Figure 14 the anvil from the band of more active cells visible in the earlier PPI is only 2km away from the daughter cell. The maximum echo in this anvil is about 20dBZ, and Figure 15 shows that by 1618-20 it had merged with this developing cell which now has a maximum echo of 65dBZ. The Z_{DR} in this Figure is quite revealing. At 30km range the positive Z_{DR} is confined to regions below the freezing level indicating ice above, but at 33km the positive Z_{DR} extends to a height of 4km with a maximum of 5dB at 2.3km altitude; above this there is a region of negative Z_{DR} with a peak value of -1.4dB occurring at 5km where Z is 62dBZ . These various regimes of Z_{DR} can be clearly identified in the vertical profile of Z and Z_{DR} passing through this region of negative Z_{DR} which is displayed in figure 16. Above 6km Z is high and Z_{DR} is very close to zero, and this probably results from tumbling graupel and hail pellets, below the freezing level (3.2km) Z_{DR} increases rapidly and this is consistent with large raindrops or large oblate melting

hydrometeors.

Negative values of Z_{DR} such as those between 3.2 and 6km in figure 16 have not been previously observed with the Chilbolton radar. In Section 4 we will analyse all possible effects which could give rise to artificial spurious values of negative Z_{DR}, but if for the moment we assume that the data is valid, then the ony plausible explanation is that this negative value is due to oblate or concical hailstones falling with some degree of alignment so that on the average the vertical diameter is about 20% greater than the vertical. This feature is very localised and quite transitory. No negative values of Z_{DR} can be found at the neighbouring azimuths only 1km away, and in the previous RHI at the same azimuth as Figure 16 there is just one gate showing a negative value of -0.7dB.

The major evolution appears to be similar to the 7 July case previously described , in that a cell having low Z but high Z_{DR} grew very rapidly. The highest value of Z observed in the cell increased from 31dB to 65dBZ in only 12 minutes.

3(c) 22 August 13.58 to 14.14

The evolution of an isolated shower on this day is shown in Figures 17,18 and 19. Sonde ascents showed that the wind was again very light at all levels and that the freezing level was about 3.1km. The convection was of quite limited depth with the 20dBZ echo contour never rising above 6.6km altitude, but in spite of this the plots show the development of an intense echo of over 60dBZ which is associated with a Z_{DR} of 8.3dB, the highest yet recorded with the Chilbolton radar.

The first RHI through the most intense part of the isolated developing cell obtained at 1358-40 is displayed in Figure 17 and

shows a large area above the freezing level where values of Z_{DR} exceed 4dB and Z is 40dBZ. The echo top (20dBZ) is at 5.6km, but above 5km values of Z_{DR} are essentially zero. Although the high values of Z_{DR} extend down to the ground the values of Z are much less at these lower altitudes, indicating that the major part of the precipitation is still above the zero degree isotherm but that a few large precipitation particles are reaching the ground. Six minutes later, as shown in Figure 18, the values of Z in the centre of the cell reach over 63dBZ but the echo top at this azimuth is only 5km. These high values of Z were accompanied by a Z_{DR} value of 8.3dB at one gate. This gate was at 2.8km altitude, very close to the freezing level, and was situated in the centre of a region 900m wide and 600m deep where Z_{DR} was above 6dB.

On this day the winds were very light and , in the absence of shear, the intense echo in Figure 18 fell to ground and the cell decayed. The compact region of Z_{DR} above 6dB fell 1km by the time of the next RHI 140 seconds later, and after a further 140 seconds it was just discernible 1.2km lower at an altitude of only 600m. By this time Z_{DR} was everywhere zero above the freezing level, with positive values confined to altitudes below 3km. This is the pattern usually observed with mature convective storms. Figure 19 was obtained eleven minutes after Figure 18, and shows that the highest values of Z_{DR} were only 2dB where Z was above 50dBZ implying raindrop size distributions much closer to the Marshall-Palmer. From Figure 3 if N_0 is 8000 m^{-3} mm^{-6} then the contours of 1dB and 2dB in Z_{DR} should be near to the contours of 35dBZ and 48dBZ respectively. This approximates to the situation in Figure 11.

4. POSSIBLE ARTIFACTS IN DIFFERENTIAL REFLECTIVITY MEASUREMENTS.

Before embarking upon an interpretation of the rather unexpectedly high values of Z_{DR} reported in the above convective clouds, we consider whether these observations could have been influenced by any possible spurious factors. Beard et al (1983) have suggested that raindrops oscillate and that their mean shape is slightly more spherical than the equilibrium one; if this effect was significant then a given value of ZDR should correspond to an even larger raindrops size than that assumed in this paper.

We now examine the effect of side lobes in the presence of reflectivity gradients. The symbols superposed on the five Figures showing the vertical profiles represent each separate data point recorded for every quarter degree increment in antenna elevation. This angular resolution is equal to the beamwidth of the Chilbolton antenna. In all these profiles changes in reflectivity of 20dBZ never occur over such small angular changes, so for the Chilbolton antenna, the signal detected by the side lobes is always much less than that sensed by the main beam. Consequently the contribution to the measured differential reflectivity by any mismatched polarisation characteristics of the sidelobes is negligible. It is also clear from Figure 16 that the negative values of Z_{DR} coincide with the maximum values of Z of over 60dBZ. Similarly the maximum values of Z_{DR} in Figure 12 occur where Z attains its highest value. If these features in Z_{DR} were artifacts due to side lobes then they should be found where Z is changing rapidly.

Differential attenuation can result in an apparent reduction in the values of Z_{DR}. If large oblate precipitation particles lie between the cell and the radar antenna, then the incident

horizontal radiation will be attenuated by more than the vertical and, consequently, the received power reflected even from spherical particles will be less in the horizontal than in the vertical, leading to an apparent negative value of Z_{DR}. In Figure 14, where we have tentatively ascribed the negative Z_{DR} to conical hail, there is no echo between the cell and the antenna and so differential attenuation cannot be responsible. It is worth commenting that even using 10cm radiation this effect can occasionally be important,but is a sensitive function of the oblateness of the intervening precipitation. Calculations assuming an exponential raindrop size distribution show that for a rainfall of 100mm/hr having a ZDR of 1dB the differential attenuation is only 0.01dB/km, but if ZDR is 3dB then the differential attenuation is increased tenfold. These figures are an order of magnitude higher at 5.6cm. Negative values of ZDR of below -0.2dB can be detected in the PPI in figure 11, at a range of 29 to 30km and a lateral range of -7km; the lowest value recorded being -0.6dB at one gate. The radiation between this region and the antenna has traversed a 2km region having a Z of over 50 dBZ and a differential reflectivity above 3dB. A differential attenuation of 0.1dB/km can account for the slightly negative values of ZDR. In none of the other sections discussed is this effect important.

The observation in mature intense convective storms that the values of Z_{DR} are so close to zero for all values of Z up to 65dBZ gives us additional confidence that there is no systematic bias between the processing of the signals of the vertical and horizontal polarisations. We conclude that the reported differential reflectivity observations are valid.

5. INTERPRETATION OF THE 1983 RESULTS.

The three evolutions described in Section 3 are the examples where the echoes were located and observed at an early stage in their growth. The most striking aspects of the evolution are the occurrence of high positive values of Z_{DR} accompanied by fairly modest values of Z as shown in Figures 5, 12 and 17. In view of the arguments advanced in Section 2 we believe that these high values of Z_{DR} imply large particles. In the early stages the high values of Z_{DR} occur both below and above the zero degree isotherm indicating that they are probably large raindrops. If they were due to wet ice particles either in wet growth or melting, then they would not be expected to be more oblate than a raindrop of the corresponding size. We shall offer an explanation assuming that these high values of Z_{DR} are due to large raindrops, but shall retain the possibility that they are due to even larger wet ice particles.

Figure 5 and the accompanying vertical profile in Figure 6 show that in this first RHI of the 7 July example, Z values near to 30dBZ were accompanied by Z_{DR} of about 3dB. Assuming a monodispersed distribution of raindrops then Figure 2 indicates that the cloud contains drops of about 4mm diameter present in a concentration of rather less than one per cubic meter. The more realistic exponential distribution plotted in Figure 3 using Pruppacher and Pitter drop shapes predicts a value of N_0 of about 8 (instead of 8000 in the normal Marshall Palmer distribution) and a rainfall rate of 0.2 mm/hr. Even with the more oblate drop shapes of Cooper et al N_0 is 40 and R is 0.35 mm/hr. The first RHI obtained in the 6 July example in Figure 12 and the profile in Figure 13 again show a Z of slighlty less than 30dBZ where Z_{DR}

is just above 3dB. These observations again suggest, using either the monodispersed or exponential model that there is a very low concentration of large (above 4mm) supercooled raindrops present in the cloud. In this case the rainfall rate is considerably less than 1mm/hr, whereas an empirical Z-R relationship would indicate about 2.5mm/hr.. The example on the 22 August shows a similar deviation from the Marshall-Palmer distribution. In the centre of the echo is a large area having Z values of about 40dBZ occurring where Z_{DR} is about 4dB, suggesting a mean raindrop size of 5 or 6mm. Figure 3 shows that this data cannot be fitted to an exponential raindrop size distribution if the Pruppacher and Pitter drop shapes are used, but a fit is possible using the more oblate shapes of Cooper et al, and implied values of N_o are at least two orders of magnitude lower than the Marshall-Palmer value.

The sizes and concentration of raindrops calculated above relate to the region of the cloud where the reflectivity is a maximum; in other parts of the cloud the implied concentrations are even lower. Evaporating rainshafts could lead to small concentrations of large drops, but these should be fairly local phenomena not occurring near the reflectivity maximum of a developing cloud. Such a low concentration of large drops would be difficult to confirm with aircraft because the cloud is evolving very rapidly and conventional probes would not obtain a statistically significant sample in a single 1 or 2km penetration.

The evolution which emerges from this limited study is rather unusual. A small number of large (4mm) drops form, which are liquid even at -10^{o}C. Rapid intensification of the echo follows,

with Z rising at a rate of up to 30dBZ in ten minutes, with subsequent glaciation and disappearance of positive values of Z_{DR} above the zero degree isotherm. The most rapid upward growth of the echo at a velocity of about 10m s^{-1} appears to coincide with partial glaciation, although values of Z_{DR} are mostly zero where the temperature is below freezing, there is a small column of positive Z_{DR} extending to an altitude where the temperature is about -10°C. This column is a transitory phenomenon persisting for less than ten minutes; it is of circular cross section with a diameter of between 1 and 2km, but the values of Z_{DR} typically reach 4dB within the column. As the cell loses its vigour the echo descends and the area of high Z_{DR} also subsides towards the ground without any very marked change in its magnitude.

It seems reasonable that a rapidly rising parcel of moist air could rise to an altitude where the temperature is -10°C before any of the surrounding ice particles mix in and cause rapid glaciation. It could be argued that large ice particles in wet growth can account for these observations, although their presence would be equally difficult to explain at these early stages of cell growth, but as suggested before, the surplus water should be shed and not lead to large positive Z_{DR}. Furthermore as the particles fall and melt, the value of Z_{DR} should rise even further and this is not observed.

Once the clouds in this study glaciate the ice particle spectrum will intially be similar to the raindrop spectrum. Federer and Waldvogel (1975) report mean spectra for hail of size less than 22mm having an average N_o of 12.1m^{-3} mm^{-1} and a D_o of 8.73mm. Similar values of D_o and N_o are apparent from Figure 3 for the initial raindrop spectra in these three examples. There

is some evidence from aircraft penetrations of developing cells (Musil et al, 1976) that the value of N_0 may be as low as 10 or 100 m^{-3}. If even smaller concentrations of large supercooled raindrops do exist in the early stages of precipitation development then they would be the natural favoured embryos which could then grow rapidly into hail without exhausting the supply of liquid water. Consequently the requirement of embryo sorting (Browning, 1978) for hail growth may not be quite so stringent. Macklin et al (1960) found that most hailstones collected in England had clear growth centres suggesting large frozen drop embryos.

In one example we infer that large hail causes a negative value of Z_{DR}, although this seems to be a rare occurrence. More normally the value of Z_{DR} is nearer to zero, indicating that hail tumbles as it falls or is asymmetric. A much more reliable hail signature at low altitudes in the cloud is a region of zero Z_{DR} where Z is very high, instead of the more normal postive Z_{DR} in heavy rain (Illingworth et al, 1986).

6. CONCLUSION.

From a study of a number of vigorous isolated convective storms over the UK during the summer of 1983 we draw the following tentative conclusions.

a) Isolated weak echoes having moderate Z but accompanied by large positive differential reflectivity (Z_{DR}) are likely to intensify very rapidly.

b) These anomalous low Z/ high positive Z_{DR} first echoes indicate very low concentrations of large precipitation particles. Although we cannot rule out the possibility that they

are large ice particles in wet growth this seems most unlikely, and we propose that they are large (~4mm) supercooled raindrops. Present theories of precipitation development do not predict the appearance of these large drops at such an early stage.

c) Such low concentrations of large drops could be very efficient hail embryos growing to large hailstones after freezing because of the lack of competition for the cloud water. This may relax requirements for embryo sorting.

d) Narrow columns of positive Z_{DR} extending by up to 2km above the zero degree isotherm occur during vigorous convection when the echo top is rising rapidly and tend to preceed high values of Z. They are generally circular in cross section of diameter between 1 and 2km, the remainder of the cloud at these heights having Z_{DR} values very close to zero. We believe that these columns may be due to large supercooled raindrops in an ascending updraught, and that their subsequent disappearance indicates rapid glaciation.

Further data sets obtained with the Chilbolton radar should provide more evidence on the size, concentration and types of hydrometeors during the evolution of convective clouds. The measurement of additional polarisation parameters should provide definite confirmation of the phase of the scattering particles.

7.ACKNOWLEDGEMENTS

This research was supported by the Meteorological Office, by NERC grant GR3/5896 and by AFOSR-85-0188. Computing facilities were provided by SERC under GR/D69372. We thank J Caylor for assistance with the Figures. This paper was written while A.J.Illingworth was a British Council/Mombushu visiting scientist with Prof Kikuchi of the University of Hokkaido, Japan.

REFERENCES

Bader, M J, Clough, S A, and Cox, G P	1986	Aircraft and dual polarisation radar observations of hydrometeors in light stratiform precipitation. Submitted to Quart. J.R. Met Soc.
Beard, K V, Johnson, D B, and Jameson A R	1983	Collisional Forcing of Raindrop Oscillations J. Atmos. Sci., 40, 455-462.
Beard, K V, and Jameson, A R	1983	Raindrop Canting, J. Atmos. Sci., 40, 448-454.
Bailey, I H and Macklin, W C	1968	Heat transfer from artificial hailstones. Quart. J. R. Met. Soc., 94, 93.
Browning, K A	1978	The structure and mechanism of hailstorms. Am. Met. Soc. Monograph, 38.
Browning, K A and Foote, G B	1976	Airflow and hail growth in supercell storms, Quart. J. R. Met. Soc., 102, 499-533.
Cherry, S M and Goddard, J W F	1982	Design features of dual-polarisation radar, URSI Conference, Bournemouth, United Kingdom.
Cherry, S M, Goddard J W F and Ouldridge, M	1984	Simultaneous measurements of rain by airborne distrometer and dual-polarisation radar. Radio Sci, 19, 169-176.
Cooper, W A, Bringi, V N Chandrasekhar, V and Seliga, T A	1983	Analysis of raindrops parameters using a 2-D precipitation probe with application to differential reflectivity. 21 Conf on Radar Meteorol, AMS, Boston.
Federer, B and Waldvogel, A	1975	Hail and raindrop size distributions from a Swiss multicell storm. J. App. Met 14, 91.
Goddard, J W F and Cherry, S M	1984a	The ability of dual-polarisation radar (coplanar linear) to predict rainfall rate and microwave attenuation. Radio Sci, 19, 201-8.
Goddard, J W F and Cherry, S M	1984b	Quantitative Precipitation Measurements with dual linear polarisation radar. 22nd Conf on Radar Meteorol. AMS, Boston.
Goddard, J W F, Cherry, S M and Bringi, V N	1983	Comparisons of dual-polarisation radar measurements of rain with ground-based distrometer measurements. J. App. Met., 21, 252-256.
Hall, M P M, Cherry, S M Goddard, J W F and Kennedy, G R	1980	Rain drop sizes and rainfall rate measured by dual-polarisation radar. Nature., 85, 195-198.
Hall, M P M, Goddard, J W F and Cherry, S M	1984	Identification of hydrometeors and other targets by dual-polarisation radar. Radio Sci, 19, 132-140.
Hallett, J, Sax, R I, Lamb, D and Murty, A S R	1978	Aircraft measurements of ice in Florida cumuli. Quart. J.R. Met. Soc. 104, 631-651.
Herzegh, P H and Carbone, R E	1984	The influence of antenna illumination function characteristics on differential reflectivity measurements. 22nd Conf on Radar Meteorol. AMS, Boston.
Heymsfield, A J and Hjelmfelt, M R	1984	Processes of Hydrometeor Development in Oklahoma Convective Clouds, J. Atmos. Sci. 41, 2811-2835.

Illingworth, A J, Goddard, J W F, and Cherry, S M	1986	Detection of hail by dual-polarisation radar, Nature, 320, 431–433.
Jameson, A R and Beard, K V	1982	Raindrop Axial Ratios, J. Appl. Meteorol. 21, 257-259.
Jones, D M A	1959	The shape of raindrops. J. Meteor. 16, 504-510.
Knight, C A and Squires, P	1982	Thunderstorms of the High Plains, Vol. 1 Colorado Associated University Press 282 pp.
Macklin, W C, Strauch, E and Ludlam, F H	1960	The density of hailstones collected from a summer storm. Nubilia 3, 12.
Matson, R J and Huggins, A W	1980	The direct measurement of the sizes, shapes and kinematics of falling hailstones. J. Atmos. Sci, 37, 1107-1125.
Musil, D J, May, E L, Smith, P L and Sand, W R	1976	Structure of an evolving hailstorm, Part IV: Internal structure from penetrating aircraft. Mon Wea Rev, 104, 596-602.
Pruppacher, H R and Klett, J D	1980	Microphysics of clouds and precipitation. Reidel, Dordrecht, Holland.
Pruppacher, H R and Pitter, R L	1971	A semi-empirical determination of the shape of cloud and rain drops. J. Atmos. Sci. 28, 86–94.
Seliga, T A and Bringi, V N	1976	Potential use of radar differential reflectivity measurements at orthogonal polarisation for measuring precipitation. J. App. Met. 15, 69-76.
Thwaites, S, Carras, J N and Macklin, W C	1977	The aerodynamics of oblate hailstones. Quart. J. R. Met. Soc, 103, 803-808.
Ulbrich, C W	1983	Natural variations in the analytical form of the raindrop size distribution. J Clim. & Appl. Met, 22, 1764-1775.
Ulbrich, C W and Atlas, D	1984	Assessment of the contribution of differential polarisation to improved rainfall measurements. Radio Sci, 19, 49-57.

LEGENDS

Figure 1: The values of Z_{DR} predicted from Gans scattering theory for oblate spheroids as a function of their minor to major axis ratio, (a/b). Figure axis vertical. Water - curve 1; solid ice of 0.92 g cm^{-3} - curve 2; ice air mixture of 0.5 g cm^{-3} - curve 3; and an ice air mixture of 0.1g cm^{-3} - curve 4.

Figure 2: The variation of reflectivity, Z, with differential refectivity, Z_{DR}, for a monodispersed distribution of raindrops having equivalent diameter D. R: Rainfall rate of 1 mm hr^{-1}. N: drop concentrations of 100 and 1000 m^{-3}. Solid curves Pruppacher and Pitter shapes, dotted curves shapes extrapolated from Cooper et al.

Figure 3: The variation of Z with Z_{DR} predicted for the exponential distribution of raindrops in Equation (2). Solid curves for N_o = 8000 m^{-3} mm^{-1} and R = 1 mm hr^{-1} using Pruppacher and Pitter shapes, dotted branches for the more oblate shapes of Cooper et al.

Figure 4: A horizontal section (PPI) at 2^o elevation at 1638-00 on 7/7/83 showing two isolated cells. In this and the following Figures the solid contour lines in Z are drawn every 10dBZ starting at 10dBZ, and in Z_{DR} every 1dB starting at 1dB. The broken contour line in both the Z and the Z_{DR} plots is for Z=5dBZ and serves to delineate the extent of the cloud.

Figure 5: A vertical section at 1635-40, azimuth 93^o, through the most intense part of the echo at 40km range in figure 4. Contours of Z and Z_{DR} as in Figure 4

Figure 6. A vertical profile of Z and Z_{DR} at 40.8km range, the gate where Z is a maximum in Figure 5. Below 3km altitude values

of Z_{DR} are anomalously high.

Figure 7. An RHI at 1641-10 through the cell in Figure 5 at azimuth 95° showing the development of a narrow column of positive Z_{DR} above 4dB which extends almost 2km above the freezing level.

Figure 8: A vertical profile of Z and Z_{DR} at range 39.9km through the column of positive Z_{DR} in Figure 7.

Figure 9: An RHI obtained at 1648-10 and azimuth 94° through the same cell as the previous five figures, but now Z and Z_{DR} are more typical of a mature glaciated cloud, with Z_{DR} only positive below the freezing level.

Figure 10: A vertical profile of Z and Z_{DR} at a range of 40.8km in Figure 9. Z_{DR} values are zero above 3km consistent with tumbling graupel, but become increasingly positive below 3km as the particles melt.

Figure 11: A PPI obtained at 1606-00 on 6/7/83 showing an isolated cell with unexpectedly high Z_{DR} at 30km range and 7km lateral distance, separated by 3km from an extensive area of intense echoes. An area of negative Z_{DR} at 29km range and lateral distance -7km (marked with an N) is believed due to differential attenuation and is discussed in Section 4.

Figure 12: An RHI at 1607-00, azimuth 148°, through the most intense part of the isolated cell in figure 11. High positive Z_{DR} accompanies a weak Z.

Figure 13: A vertical profile of Z and Z_{DR} at 32.1km range through the maximum Z echo in Figure 12. Comparison with Figure 3 confirms the anomalously high values of Z_{DR}.

Figure 14: An RHI at 1613-20, azimuth 146°, showing the development of a narrow column with Z_{DR} values exceeding 5dB which extends over 1.5km above the freezing level.

Figure 15: An RHI at 1618-20, azimuth 145°, through the same cell as the previous four Figures. An additional -0.5dB contour in Z_{DR} is plotted (marked with an N), and occurs where Z is above 60dBZ. The negative Z_{DR} is believed to be due to conical hail.

Figure 16: A vertical profile of Z and Z_{DR} at 33km range through the negative Z_{DR} region in Figure 14, demonstrating that the negative Z_{DR} occurs where Z is a maximum.

Figure 17: The first RHI through a developing cell at 1358-40 on 22/8/83, azimuth 78°. Note the high Z_{DR} above the freezing level.

Figure 18: An RHI through the cell in figure 17 obtained at 1404.40, azimuth 78°. The highest Z_{DR} contour is 7dB with a maximum value at one gate of 8.3dB. Echo top is only 5km.

Figure 19: An RHI obtained 11 minutes later than Figure 18 at 1415.40, azimuth 80°. The large precipitation particles have fallen to ground and Z and Z_{DR} are much closer to those expected for a Marshall-Palmer drop size distribution.

Fig 1

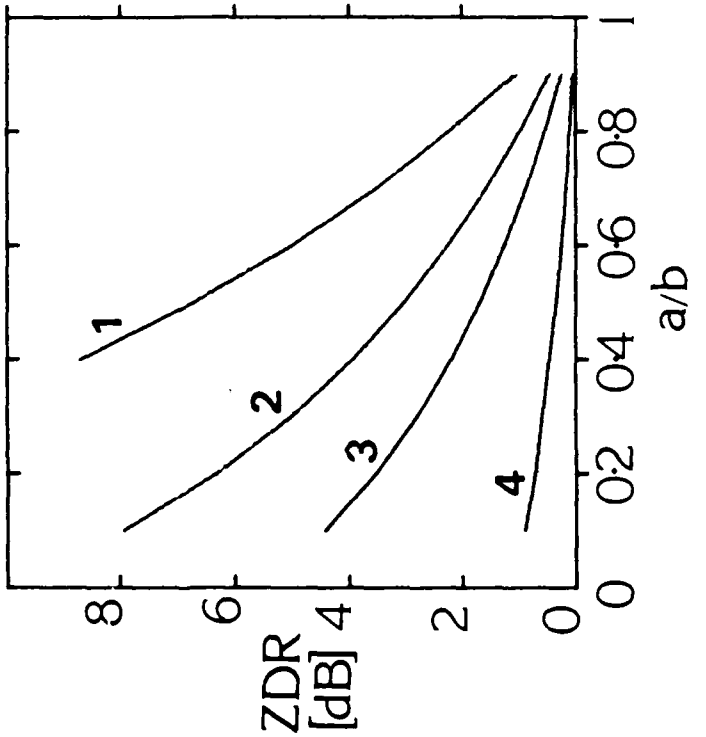

Fig 2

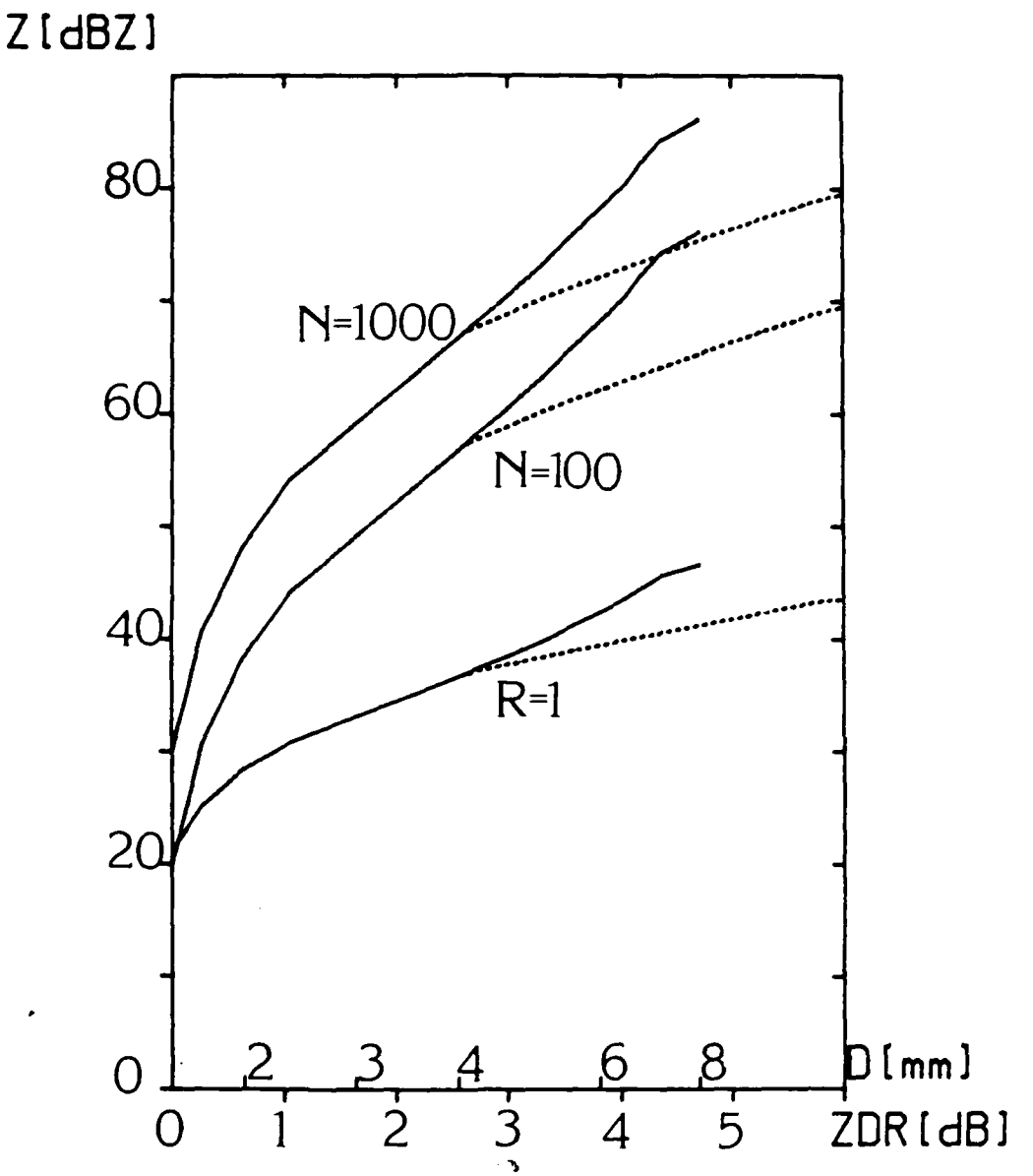

Fig 3

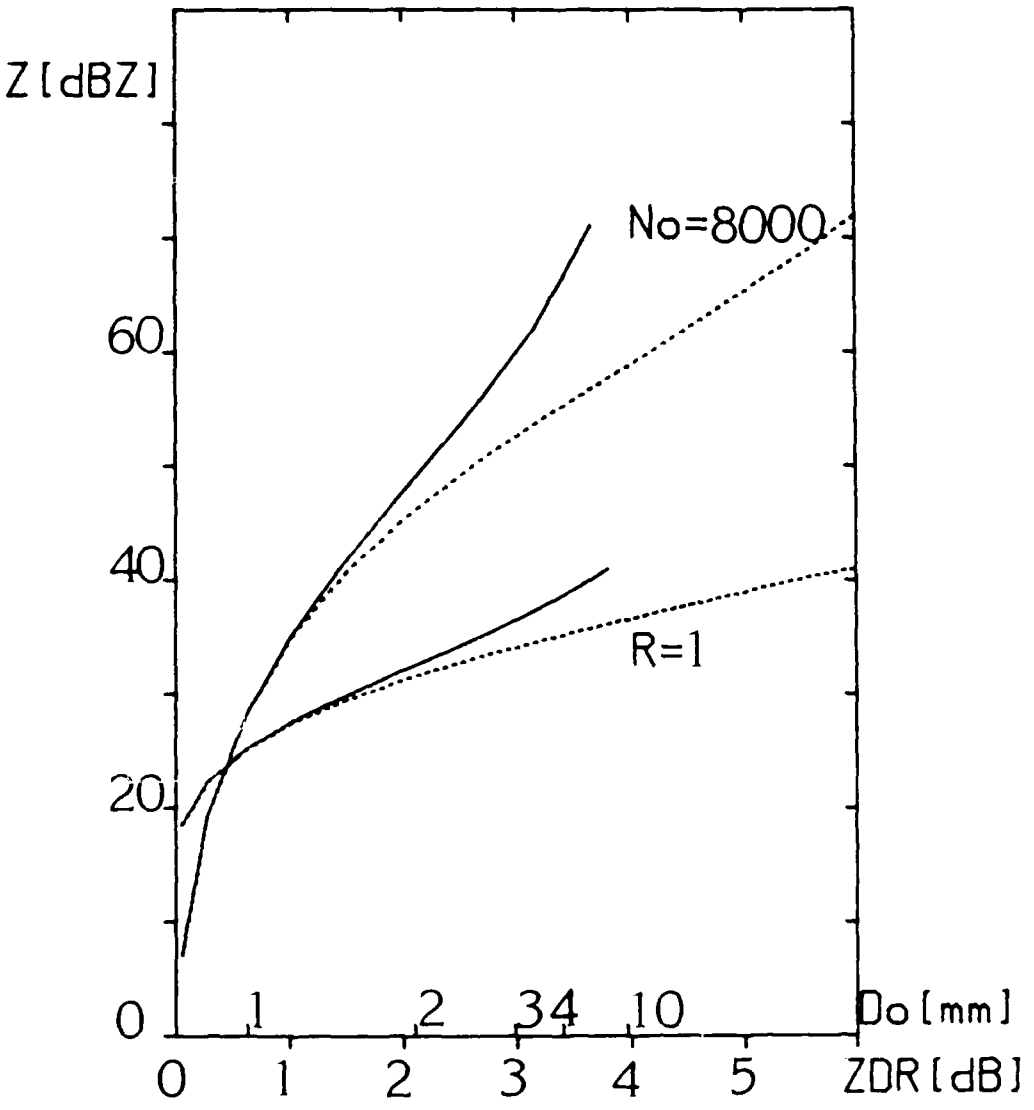

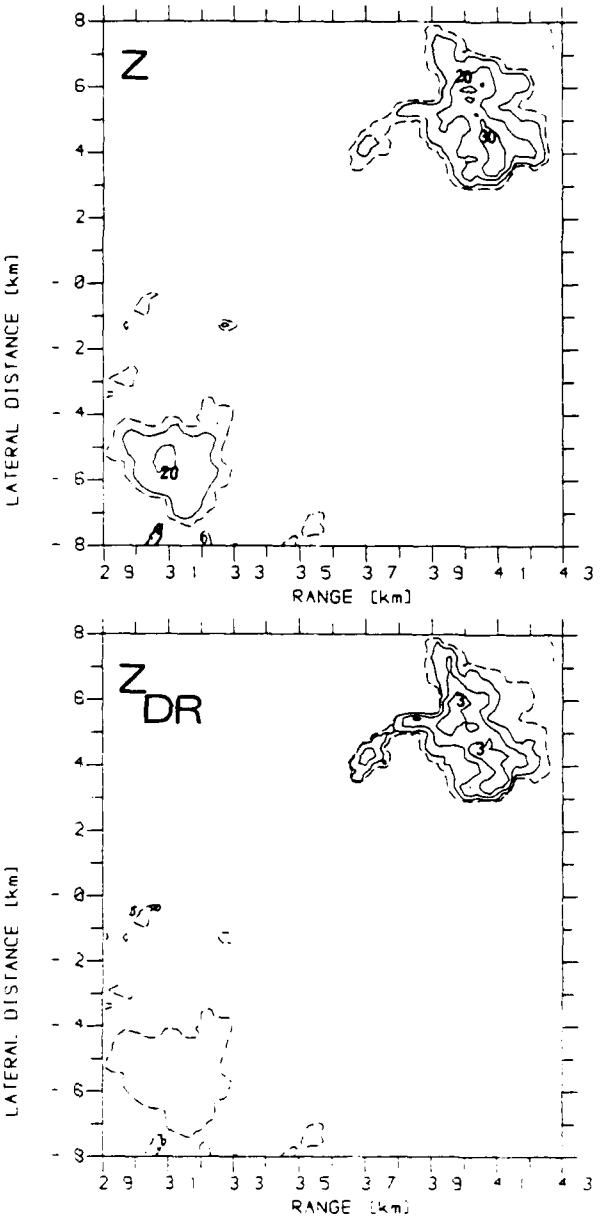
Z
20
30
20
LATERAL DISTANCE [km]
RANGE [km]
Z_{DR}
3
3
LATERAL DISTANCE [km]
RANGE [km]

Fig 5

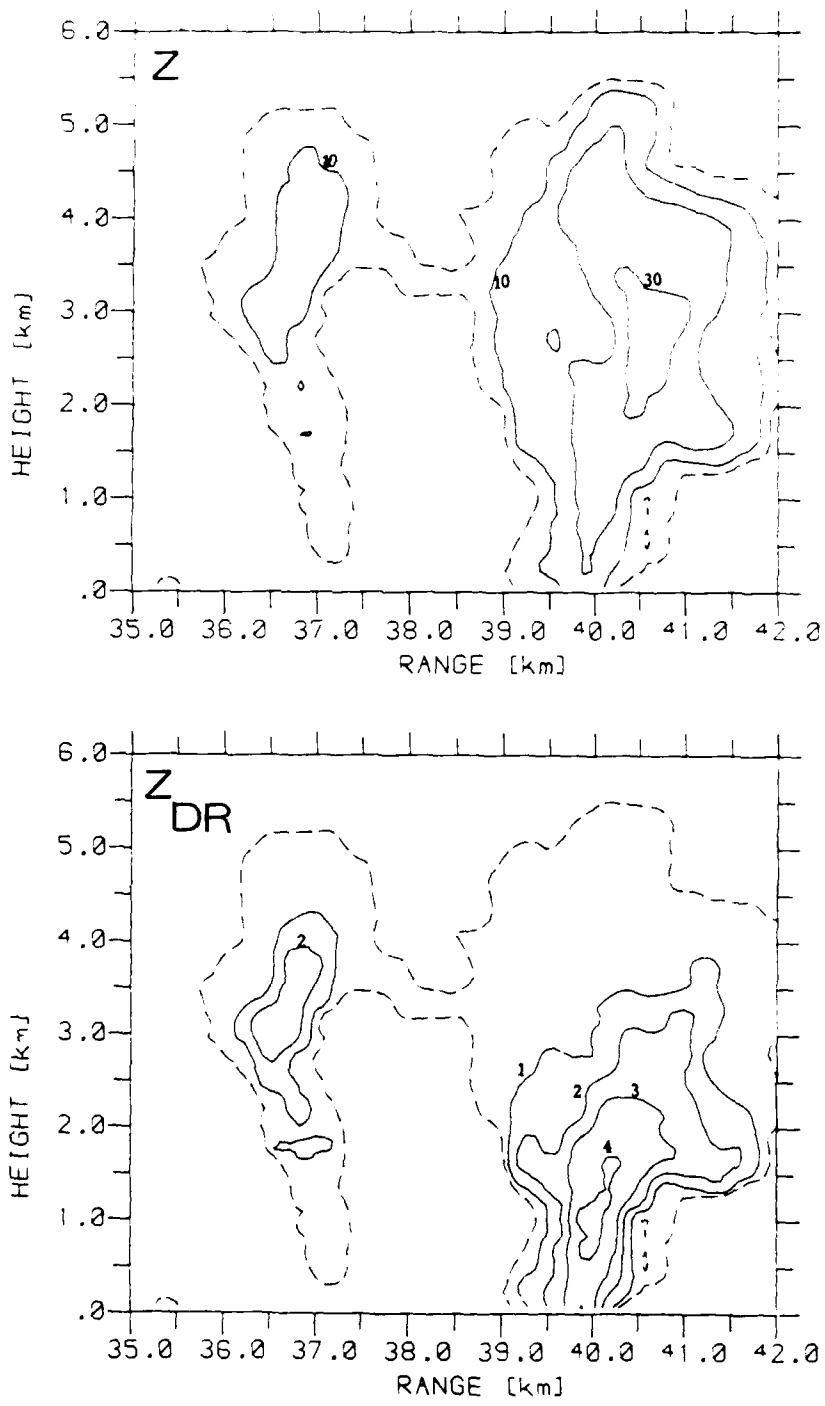
Z
6.0
5.0
4.0
3.0
2.0
1.0
.0
HEIGHT [km]
20
10
30
0
35.0 36.0 37.0 38.0 39.0 40.0 41.0 42.0
RANGE [km]
Z DR
6.0
5.0
4.0
3.0
2.0
1.0
.0
HEIGHT [km]
2
1
2
3
4
35.0 36.0 37.0 38.0 39.0 40.0 41.0 42.0
RANGE [km]

QJRMS

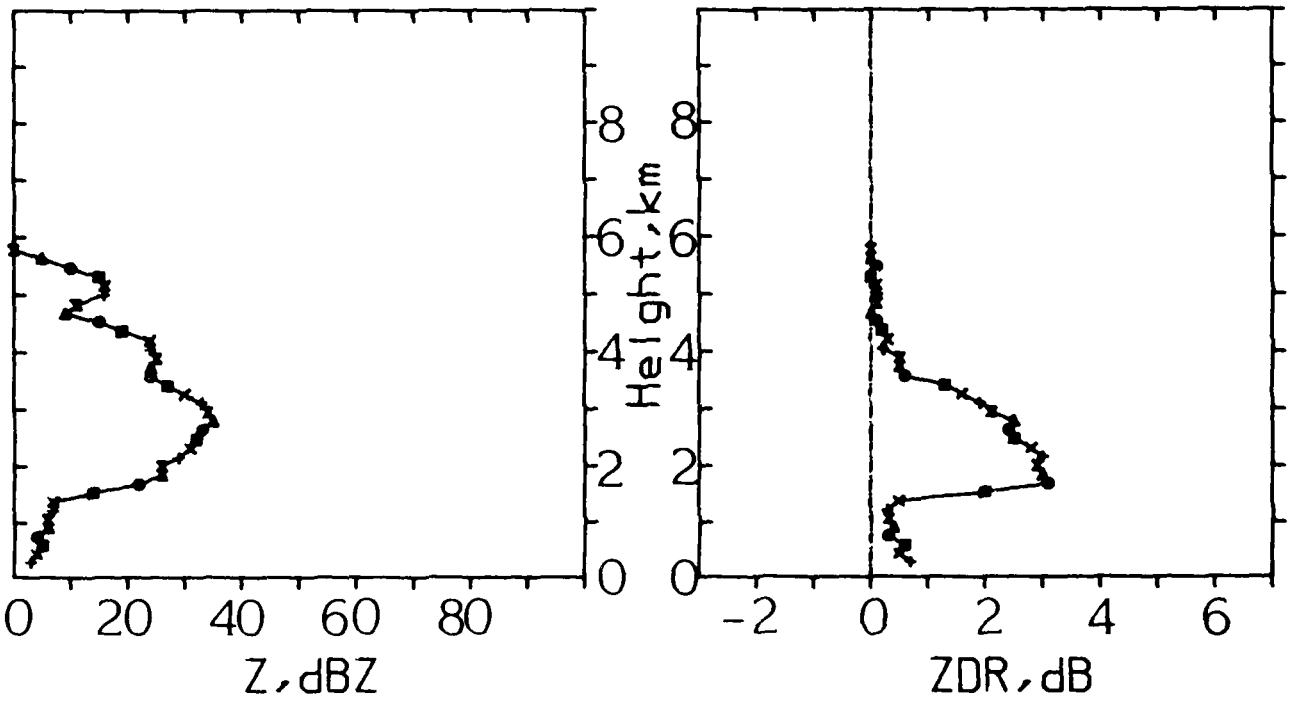

Fig 7

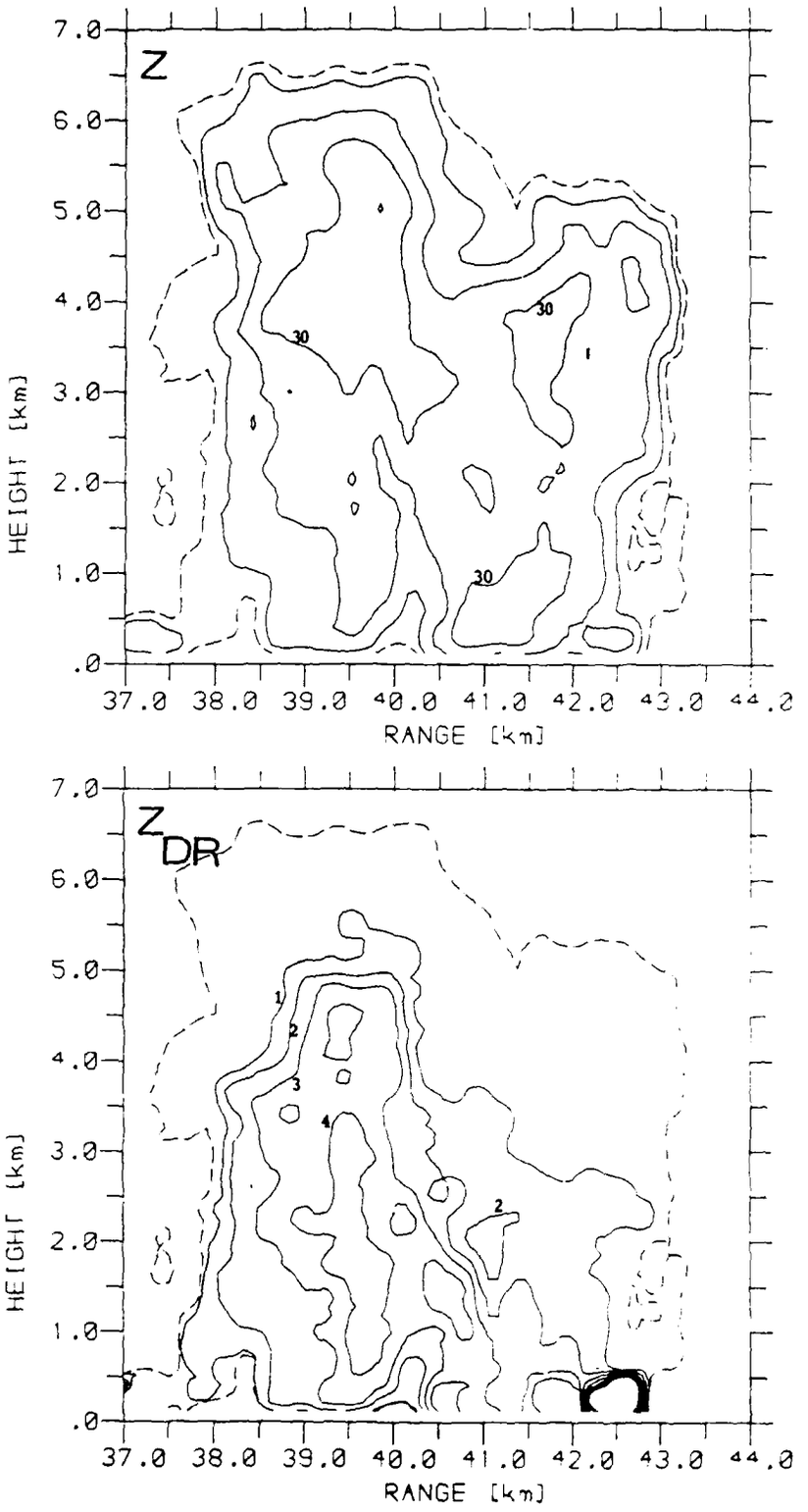
Z
7.0
6.0
5.0
4.0
3.0
2.0
1.0
.0
HEIGHT [km]
30
30
30
1
37.0 38.0 39.0 40.0 41.0 42.0 43.0 44.0
RANGE [km]
Z DR
HEIGHT [km]
1
2
3
4
2
37.0 38.0 39.0 40.0 41.0 42.0 43.0 44.0
RANGE [km]

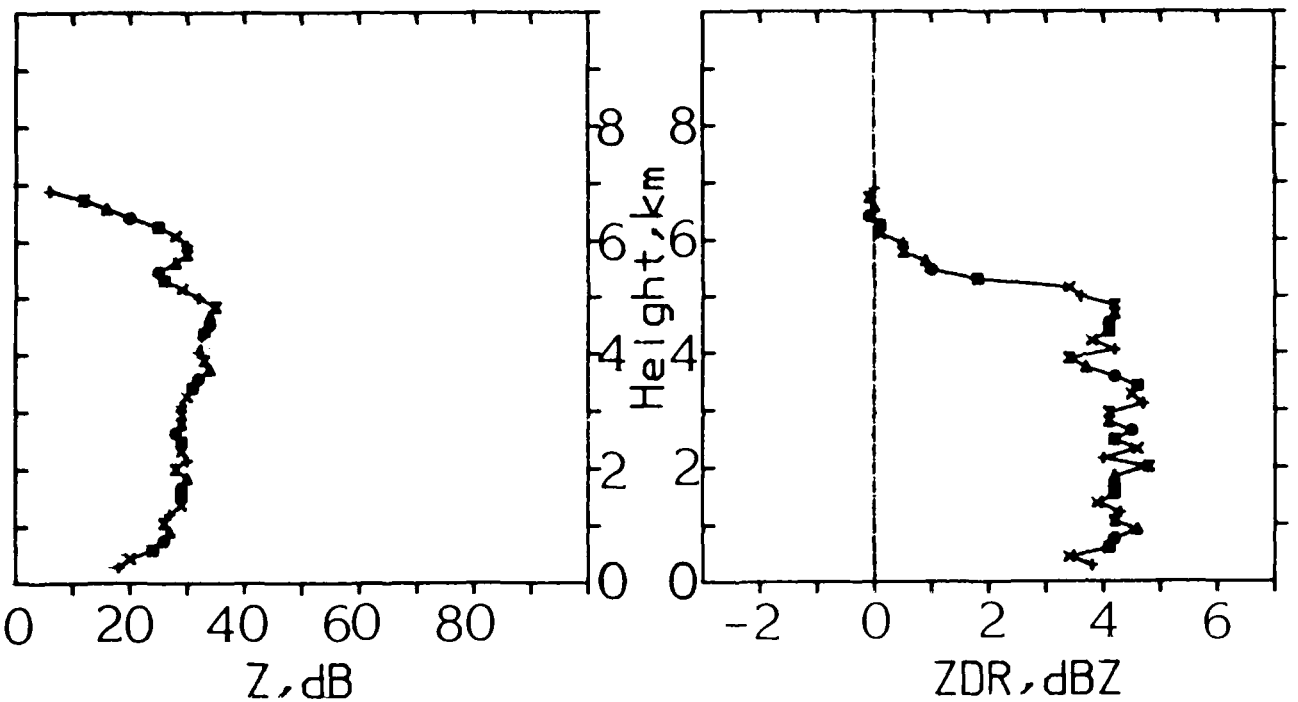
0
20
40
60
80
Z, dB
0
2
4
6
8
Height, km
-2
0
2
4
6
ZDR, dBZ

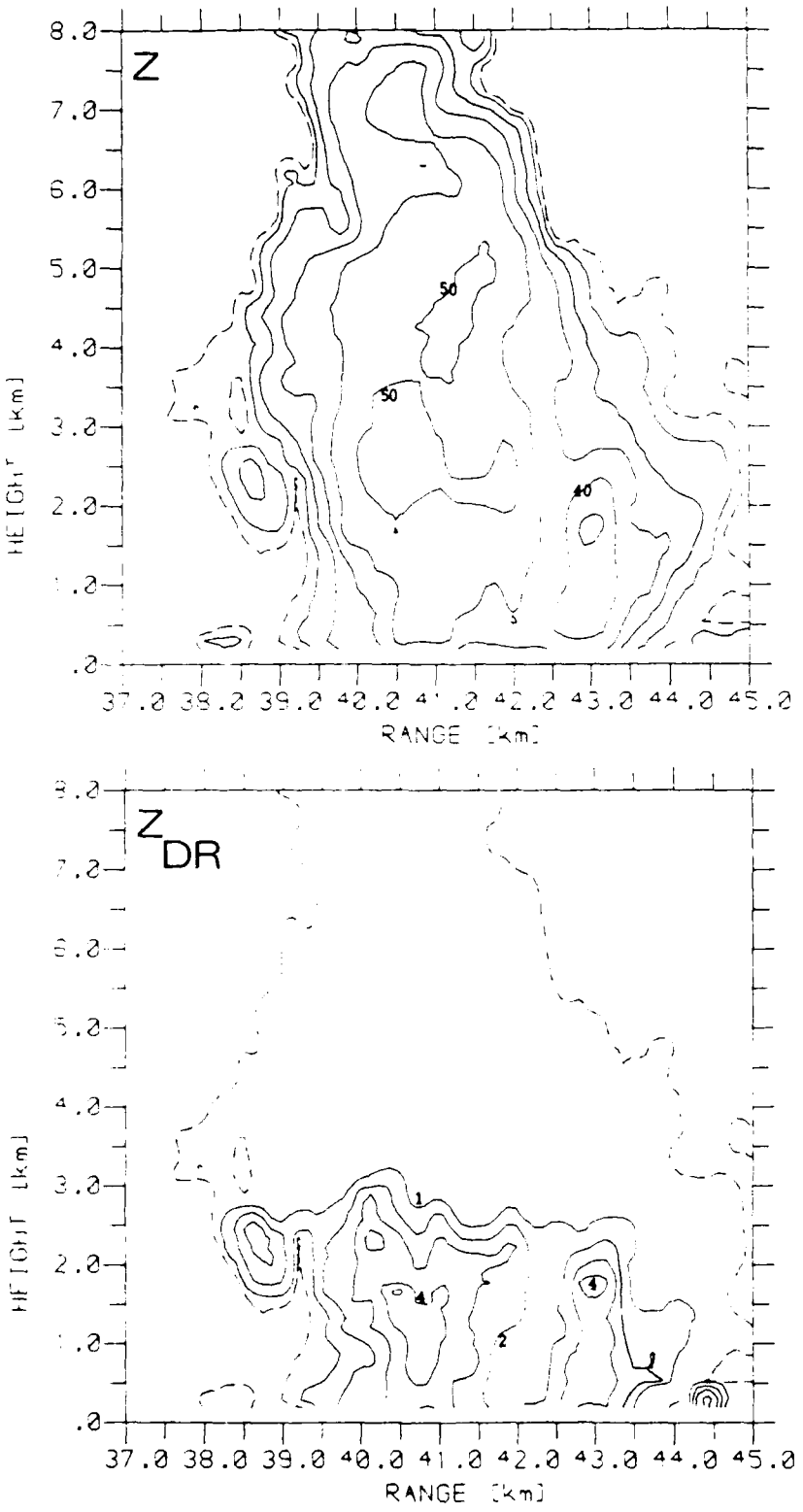
Z
8.0
7.0
6.0
5.0
4.0
3.0
2.0
1.0
.0
50
50
40
37.0 38.0 39.0 40.0 41.0 42.0 43.0 44.0 45.0
RANGE [km]
Z_{DR}
1
4
2
37.0 38.0 39.0 40.0 41.0 42.0 43.0 44.0 45.0
RANGE [km]

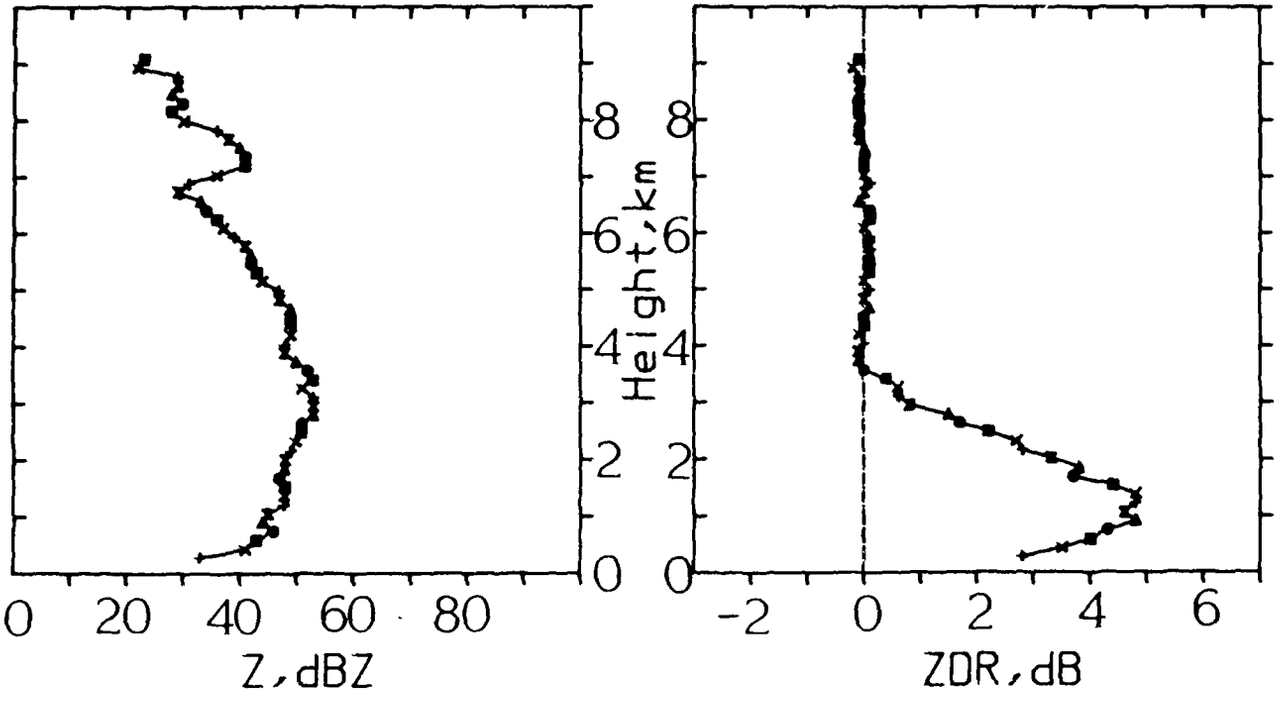
0
20
40
60
80
Z, dBZ
0
2
4
6
8
Height, km
-2
0
2
4
6
ZDR, dB

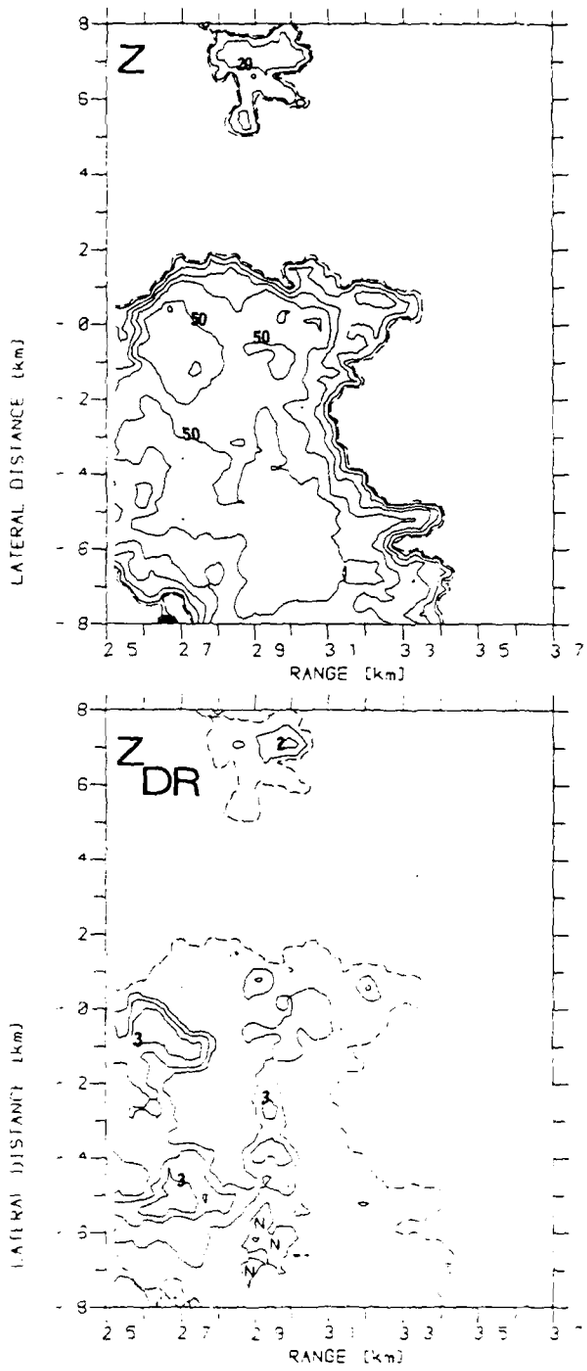
Z
20
50
50
50
LATERAL DISTANCE (km)
RANGE (km)
Z_DR
3
3
3
N
N
LATERAL DISTANCE (km)
RANGE (km)

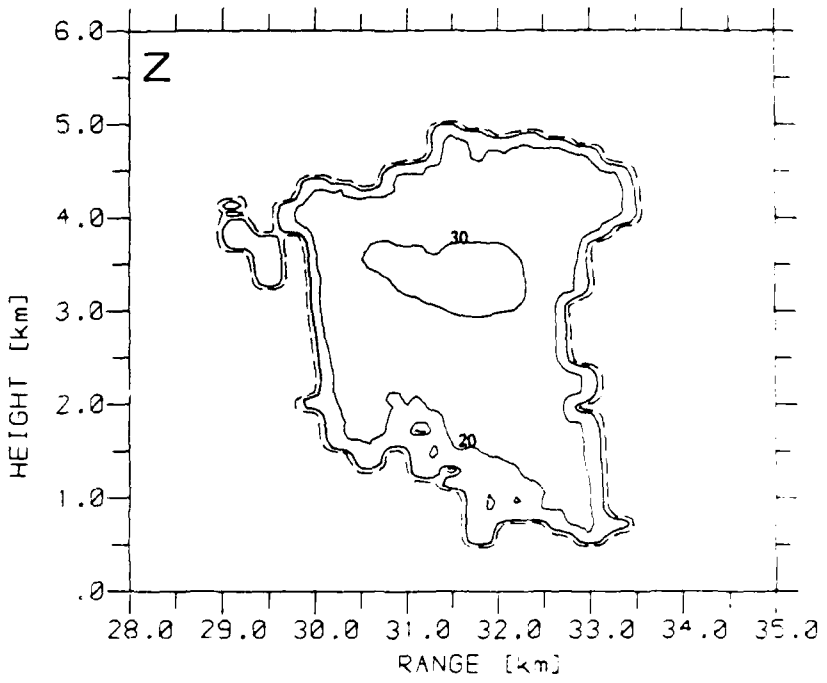
Z
6.0
5.0
4.0
3.0
2.0
1.0
.0
HEIGHT [km]
30
20
28.0 29.0 30.0 31.0 32.0 33.0 34.0 35.0
RANGE [km]

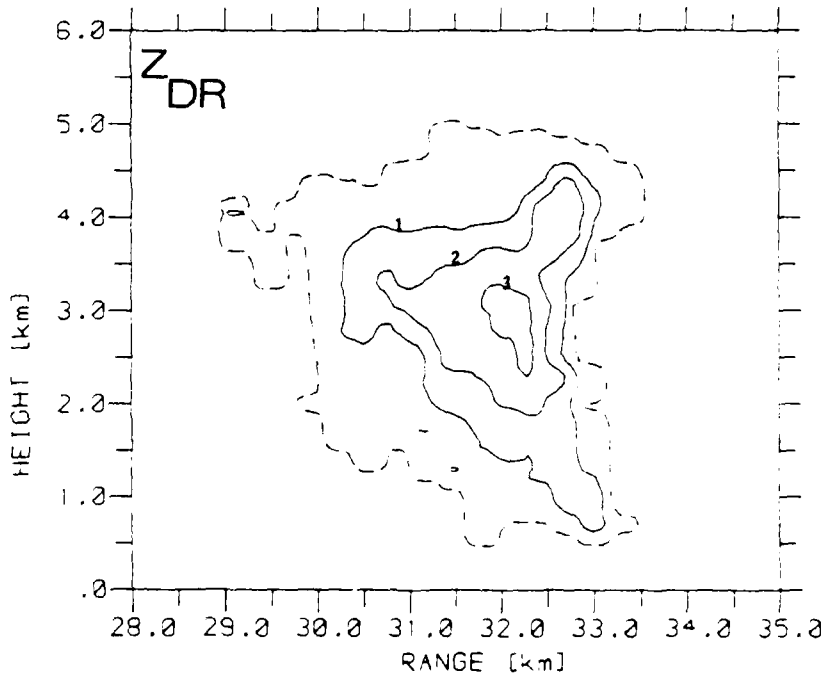
Z DR
6.0
5.0
4.0
3.0
2.0
1.0
.0
HEIGHT [km]
1
2
3
28.0 29.0 30.0 31.0 32.0 33.0 34.0 35.0
RANGE [km]

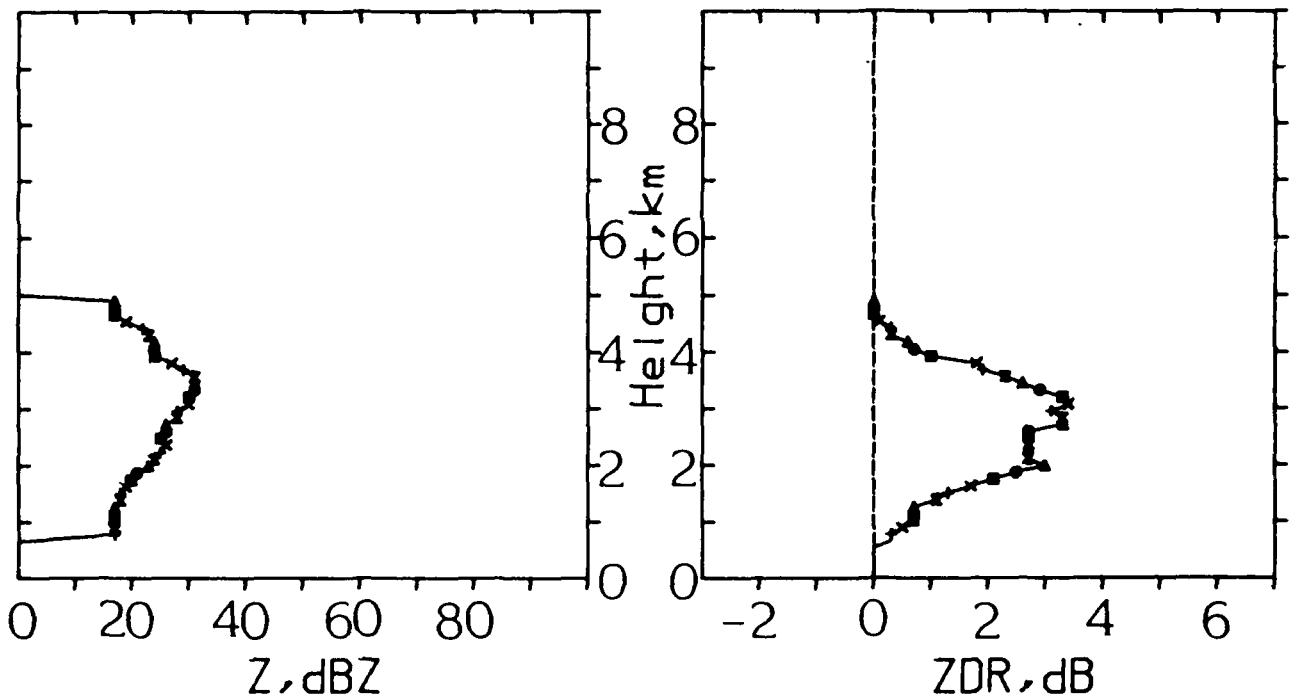
0
20
40
60
80
Z, dBZ
Height, km
0
2
4
6
8
-2
0
2
4
6
ZDR, dB

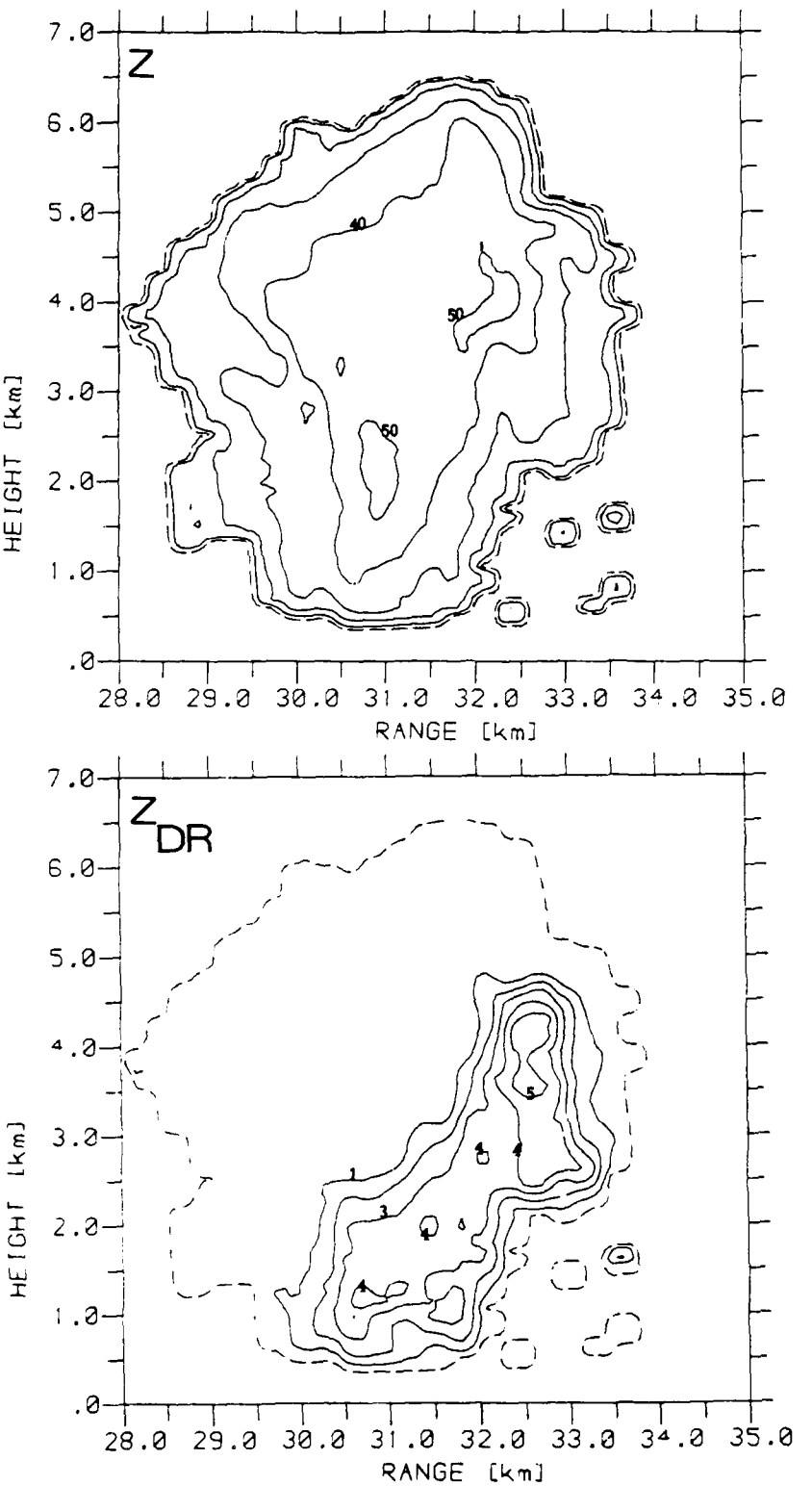
Z
7.0
6.0
5.0
4.0
3.0
2.0
1.0
.0
HEIGHT [km]
40
50
50
28.0 29.0 30.0 31.0 32.0 33.0 34.0 35.0
RANGE [km]
ZDR
HEIGHT [km]
RANGE [km]

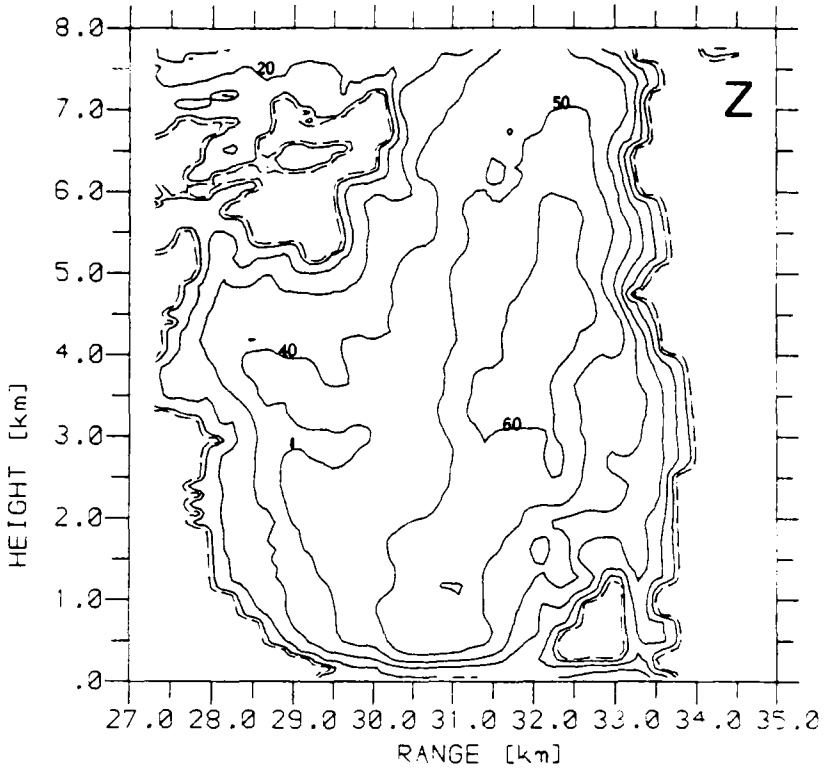
Z
20
40
50
60
HEIGHT [km]
8.0
7.0
6.0
5.0
4.0
3.0
2.0
1.0
.0
27.0 28.0 29.0 30.0 31.0 32.0 33.0 34.0 35.0
RANGE [km]

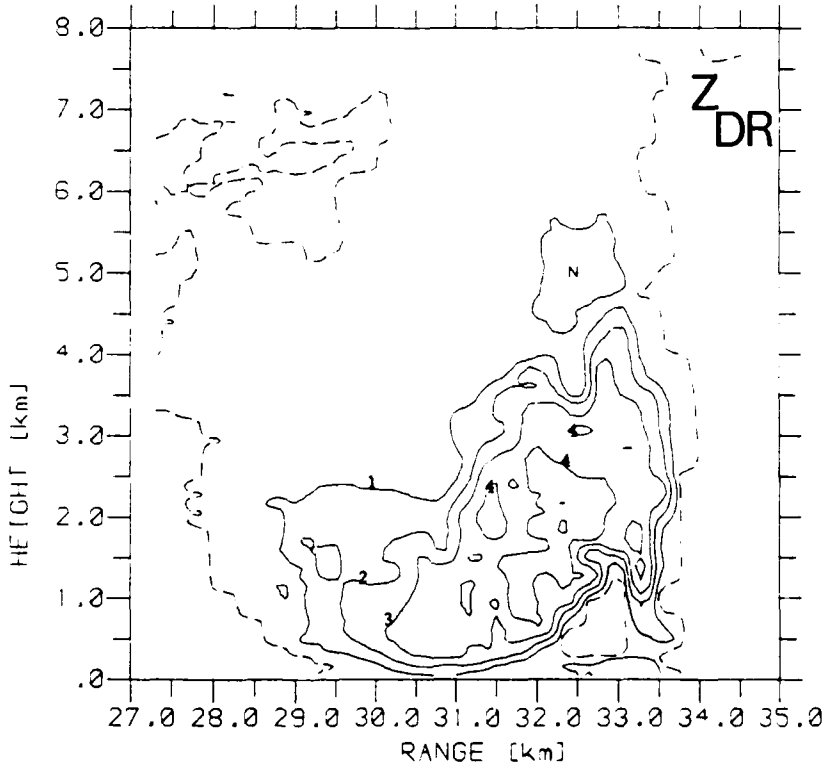
Z DR
N
1
2
3
4
HEIGHT [km]
8.0
7.0
6.0
5.0
4.0
3.0
2.0
1.0
.0
27.0 28.0 29.0 30.0 31.0 32.0 33.0 34.0 35.0
RANGE [km]

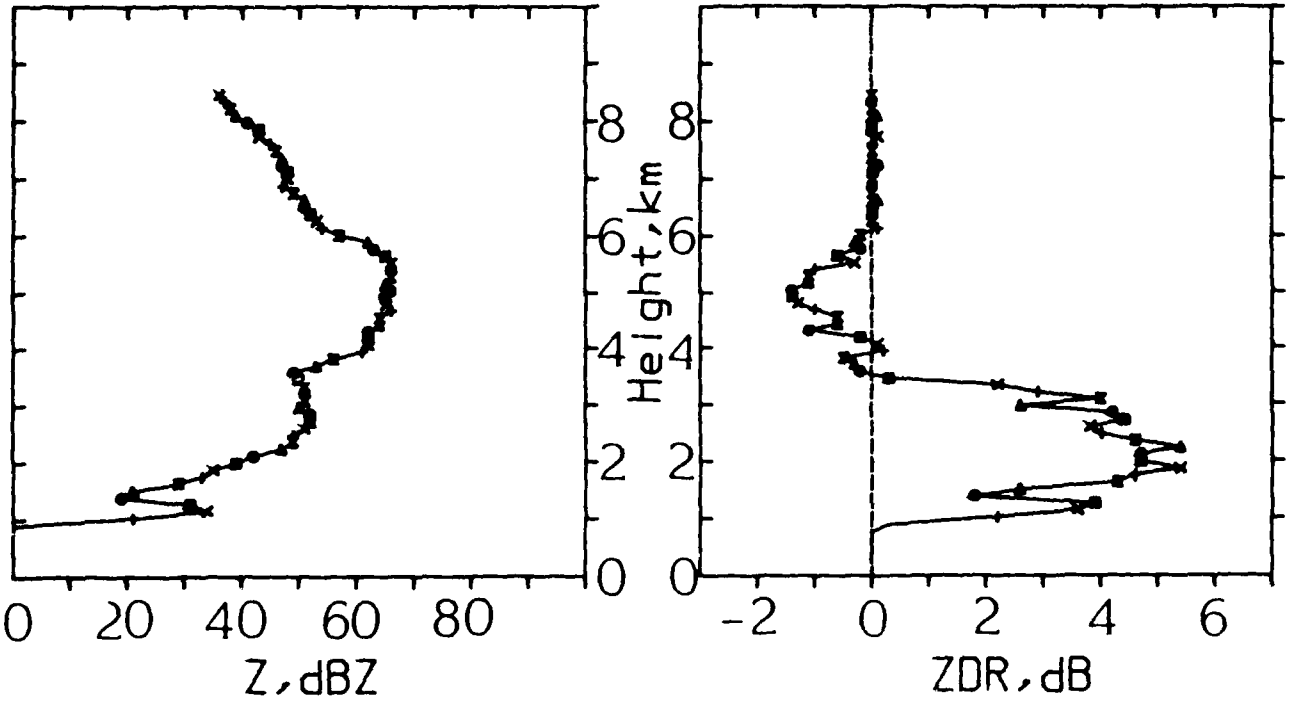
0
20
40
60
80
Z, dBZ
Height, km
0
2
4
6
8
-2
0
2
4
6
ZDR, dB

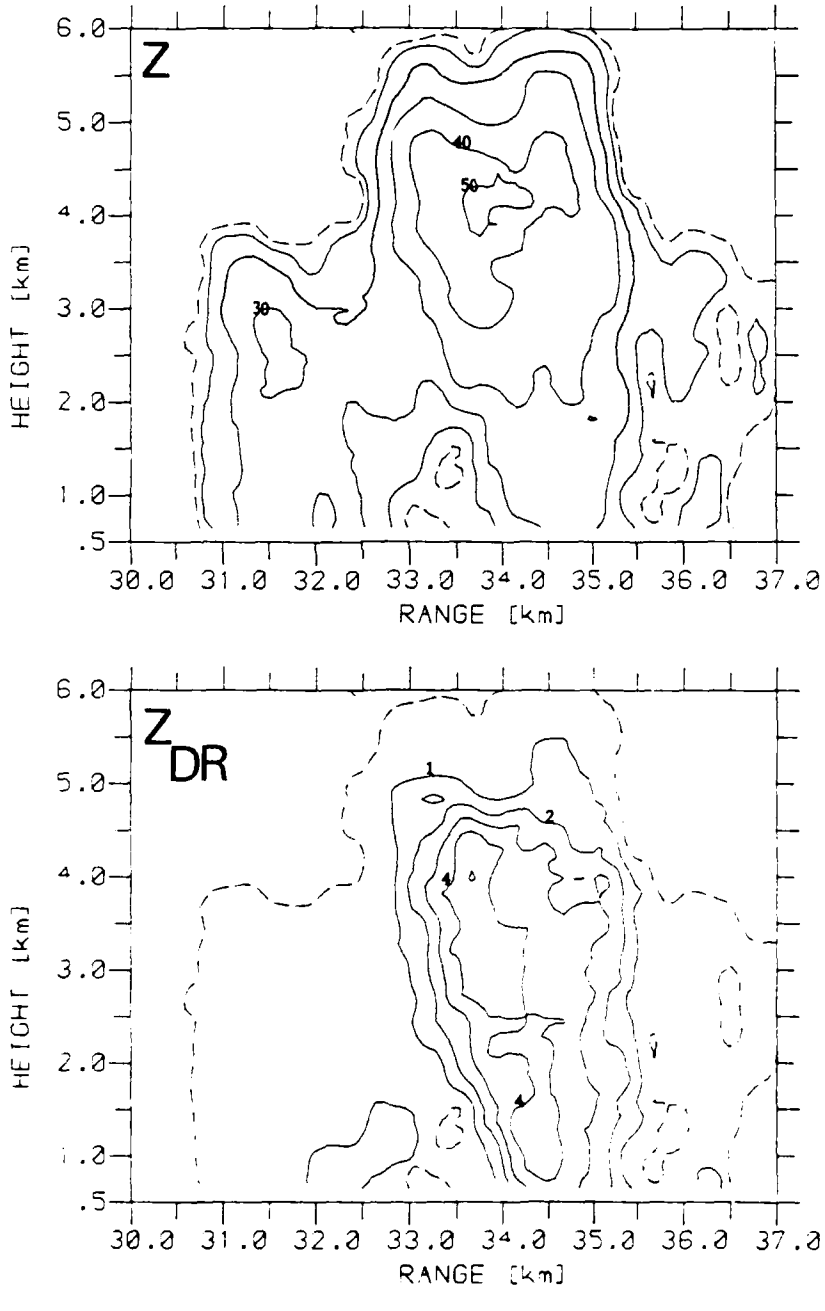
Z
6.0
5.0
4.0
3.0
2.0
1.0
.5
HEIGHT [km]
40
50
30
30.0 31.0 32.0 33.0 34.0 35.0 36.0 37.0
RANGE [km]
Z DR
6.0
5.0
4.0
3.0
2.0
1.0
.5
HEIGHT [km]
1
2
1
30.0 31.0 32.0 33.0 34.0 35.0 36.0 37.0
RANGE [km]

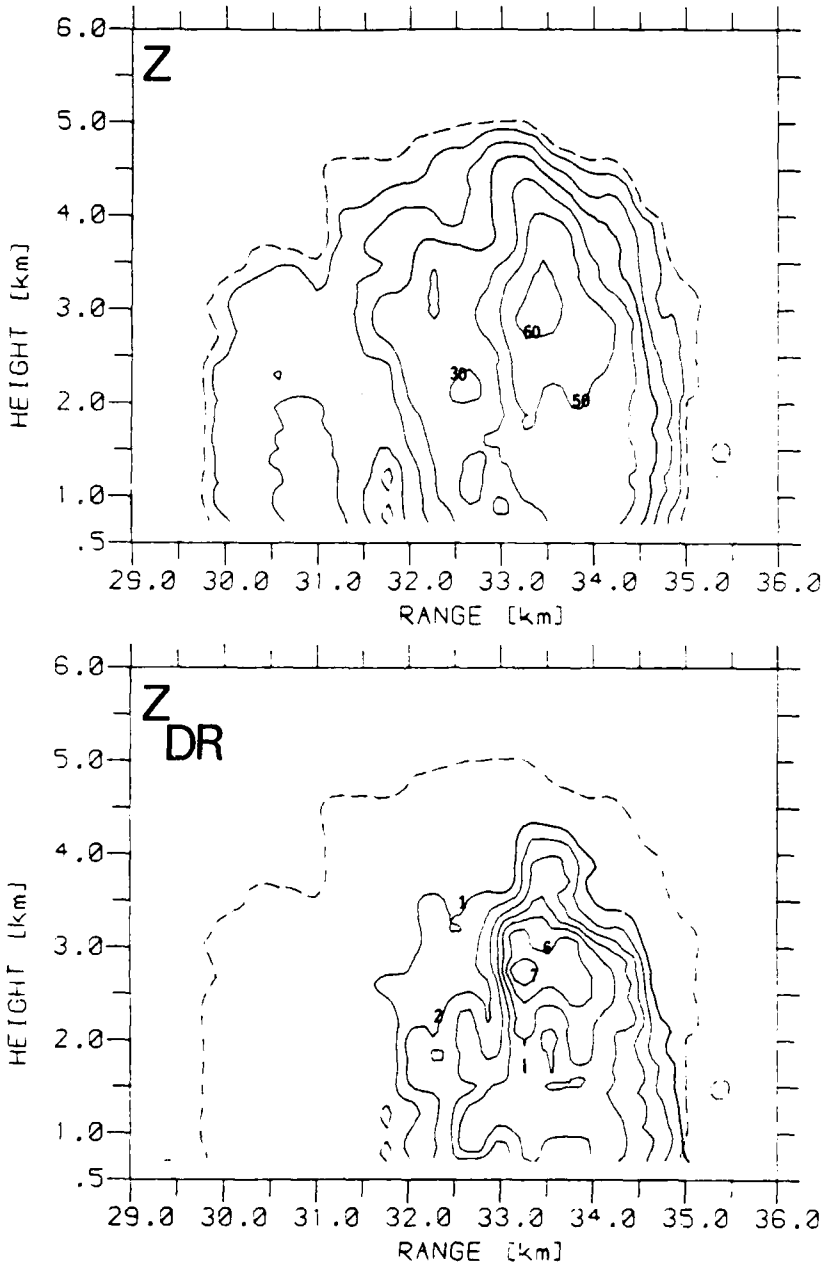
Z
6.0
5.0
4.0
3.0
2.0
1.0
.5
HEIGHT [km]
60
30
50
29.0 30.0 31.0 32.0 33.0 34.0 35.0 36.0
RANGE [km]
Z DR
6.0
5.0
4.0
3.0
2.0
1.0
.5
HEIGHT [km]
1
6
7
2
0
1
29.0 30.0 31.0 32.0 33.0 34.0 35.0 36.0
RANGE [km]

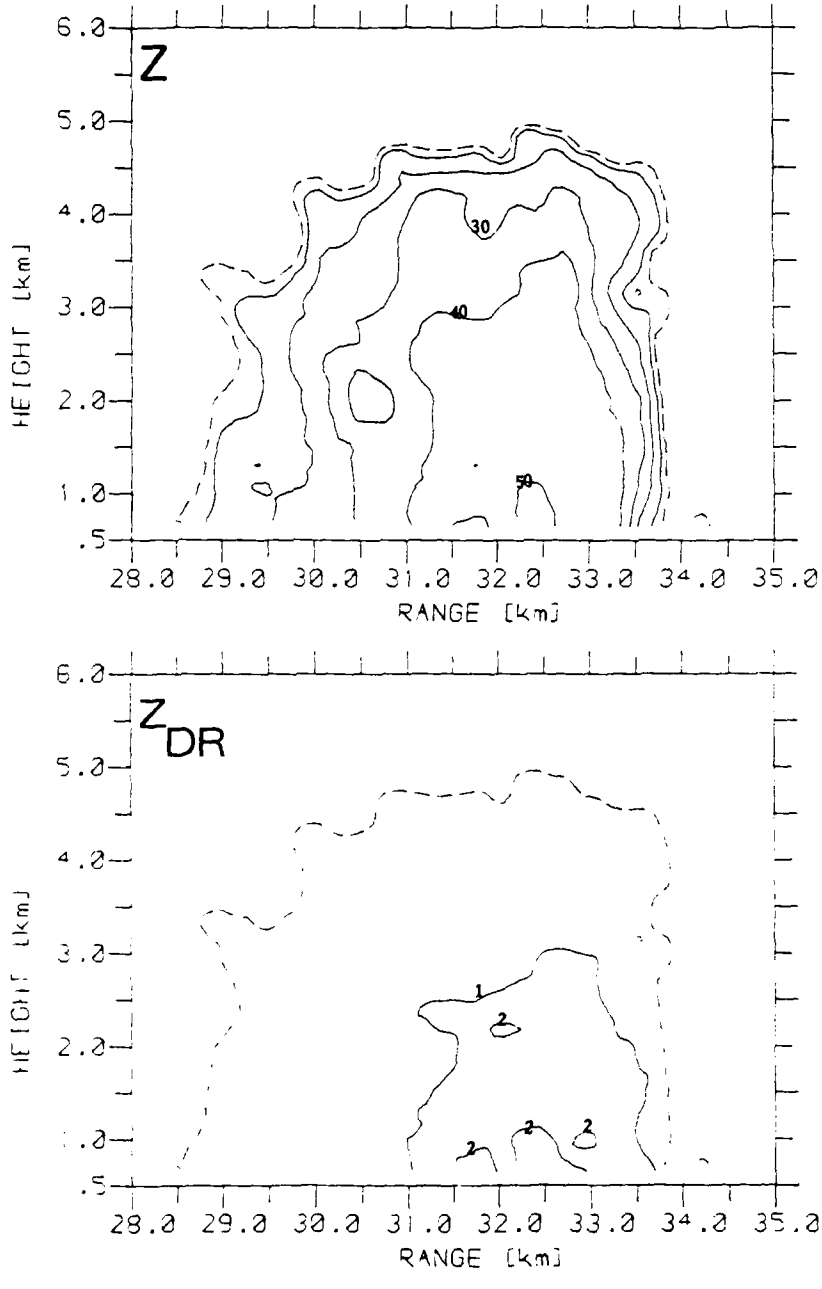
Z
6.0
5.0
4.0
3.0
2.0
1.0
.5
HEIGHT [km]
30
40
50
28.0 29.0 30.0 31.0 32.0 33.0 34.0 35.0
RANGE [km]
Z_{DR}
6.0
5.0
4.0
3.0
2.0
1.0
.5
HEIGHT [km]
1
2
2
2
2
28.0 29.0 30.0 31.0 32.0 33.0 34.0 35.0
RANGE [km]

END

DATE
FILMED
4-87

DTIC